EFFECTS OF CHRONIC INSULIN AND HIGH GLUCOSE ON INSULIN-STIMULATED RESPONSES IN HUMAN PREADIPOCYTES

By

Jason El Bilali

Thesis submitted to the

Faculty of Graduate and Postdoctoral Studies

in partial fulfillment of the requirements

for the M.Sc. degree in Biochemistry

Biochemistry, Microbiology and Immunology

Faculty of Medicine

University of Ottawa

Ottawa, Canada

ABSTRACT

The preadipocyte is crucial for healthy adipose tissue (AT) remodeling, and insulin resistance in these cells may contribute to AT dysfunction. Chronic exposure to insulin and high glucose induces insulin resistance in the 3T3-L1 mouse adipocyte cell line *in vitro*, however, whether this occurs in human preadipocytes is not known. To investigate this, human preadipocytes were isolated from subcutaneous AT obtained from 6 female patients undergoing elective surgery (Research Ethics Board-approved). Human preadipocytes were incubated in 5 mM glucose or 25 mM glucose in the presence or absence of 0.6 nM insulin for 48 hours, followed by acute 100 nM insulin stimulation. 25 mM glucose + 0.6 nM insulin inhibited insulin-stimulated tyrosine phosphorylation of IR-β (77%) and IRS-1 (81%) compared to NG ($p<0.01$), however, insulin-stimulated Ser^{473} Akt phosphorylation was not affected. 25 mM glucose and/or 0.6 nM insulin did not significantly change levels of pro-inflammatory adipokines. 25 mM glucose and/or 0.6 nM, prior to and/or during 14 days of adipogenic induction, did not affect levels of adipogenic markers or intracellular triglyceride accumulation.

ACKNOWLEDGEMENTS

First and foremost, I would like to thank my parents, Abdellah El Bilali and Lisa Coldwell, for all the support and encouragement. I would like to thank Johanna Dobransky for keeping me positive, focused, and motivated. I would also like to thank:

Dr. Alexander Sorisky: Thank you for pushing me to think critically and for teaching me to be more concise. A supervisor can make or break the graduate experience, and with this said, I am extremely grateful to have had to the opportunity to work with someone who cares so much about the success of his students.

Dr. AnneMarie Gagnon: Thank you for always taking time out of your day to answer any and every question I had. I appreciated all your guidance, support and patience throughout this project. You provided great mentorship, and I am a better scientist because of it.

Anne Landry: Thank you for all your help, positive energy, and for always ensuring the lab was well stocked.

Sorisky Lab Members: Thank you for always keeping me entertained.
- Vian Peshdary
- Arran McBride
- David Felske
- Amanda Biernacka-Larocque

George Styles and Dr. Lionel Filion: Thank you for all the great advice and guidance.

TAC Members
- Dr. Rashmi Kothary
- Dr. Zemin Yao

Funding Sources
- University of Ottawa
- Ottawa Hospital Research Institute
- Government of Ontario (QEII-GSST)

Finally, thank you to all the patients and surgeons who made this study possible.

TABLE OF CONTENTS

LIST OF ABBREVIATIONS

A

Abhd5	α/β hydrolase fold domain 5
ACC	Acetyl-CoA carboxylase
AGE	Advanced glycation end-product
ANOVA	Analysis of variance
aP2	Fatty acid binding protein 4
AT	Adipose tissue
ATGL	Adipose triglyceride lipase
ATM	Adipose tissue macrophage

B

BAT	Brown adipose tissue
BCA	Bicinchonic acid assay
BMI	Body mass index
BMP	Bone morphogenetic protein
BSA	Bovine serum albumin

C

cAMP	Cyclic adenosine monophosphate
C/EBP	CCAAT-enhancer-binding protein
CHO	Chinese Hamster Ovary

D

DG	Diglyceride
DMEM	Dulbecco's modified Eagle's medium
DNL	De novo lipogenesis
DOC	Deoxycholate

E

ECM	Extracellular matrix
ER	Endoplasmic reticulum

F

FABP4	Fatty acid binding protein 4
FAS	Fatty acid synthase
FoxO1	Forkhead box protein O1
FRET	Förster resonance energy transfer

G

G0S2	G0/G1 switch gene 2
G3P	Glyceraldehyde 3-phosphate
GLUT	Glucose Transporter

H

HSL	Hormone-sensitive lipase

I

IBMX	3-isobutyl-1-methylxanthine
IFATS	International Federation for Adipose Therapeutics and Science
IGF	Insulin-like growth factor
IGF1R	Insulin-like growth factor 1 receptor
IR	Insulin receptor
IRS	Insulin receptor substrate
ISCT	International Society for Cellular Therapy

J

JNK	c-Jun N-terminal kinases

L

LAR	Leukocyte common antigen–related
LD	Lipid droplet
Lef	Leukocyte early factor
Lox	Lysyl oxidase

M

MCE	Mitotic clonal expansion
MCP-1	Monocyte chemoattractant protein-1
MG	Monoglyceride
MGL	Monoglyceride lipase
MHO	Metabolically healthy but obese
MSC	Mesenchymal stem cell
mTORC	Mammalian target of rapamycin complex

N

NEFA	Non-esterified free fatty acid

P

PBS	Phosphate-buffered saline
PDE-3b	Phosphodiesterase-3b
PDK-1	Phosphoinositide-dependent kinase-1
PEPCK	Phosphoenolpyruvate carboxykinase
PH	Pleckstrin homology
PHLPP	PH-domain-and-Leucine-rich-repeat protein phosphatase
PI3K	Phosphoinositide 3-kinase
PKC	Protein Kinase C
PKA	Protein Kinase A
PP	Protein Phosphatase
PPAR	Peroxisome proliferator-activated receptor
PPRE	Peroxisome proliferator hormone response element

PTB	Phosphotyrosine-binding domain
PTEN	Phosphatase and tensin homolog
PTK	Protein Tyrosine Kinase
PTP	Protein Tyrosine Phosphatase

R

Rat-1 HIRcBs	Rat-1 fibroblasts overexpressing the human insulin receptor
Rb	Retinoblastoma
ROS	Reactive Oxygen Species
RT	Reverse Transcription
RXR	Retinoid X Receptor

S

SAT	Subcutaneous adipose tissue
SC	Subcutaneous
Sh	Src-homology
SRE	Sterol regulatory element
SREBP	Sterol regulatory element binding protein
SVF	Stromal vascular fraction

T

T2D	Type 2 diabetes
TCA	Trichloroacetic acid
Tcf	T-cell factor
TE	Tris-EDTA
TG	Triglyceride
TGF	Transforming growth factor
TNF	Tumor necrosis factor
Tpt1	Translationally controlled tumor protein 1
Txnip	Thioredoxin interacting protein

U

UCP	Uncoupling protein

V

VAT	Visceral adipose tissue
VS	Visceral

W

WAT	White adipose tissue

LIST OF FIGURES

INTRODUCTION

An introduction to adipose tissue

Adipose tissue (AT) is a major endocrine organ specialized in energy metabolism. Although involved primarily with regulation of lipid metabolism, AT also acts as a thermal insulator and protects against mechanical damage (Hassan et al., 2012). AT regulates energy homeostasis by storing excess energy as lipid or by releasing non-esterified free-fatty acids (NEFA) into circulation when energy is required. Furthermore, through the secretion of AT-derived factors (adipokines) into circulation, AT modulates insulin sensitivity, inflammation and whole-body metabolism (Jung and Choi, 2014).

In mammals, AT is subcategorized into two groups: brown adipose tissue (BAT) and white adipose tissue (WAT). BAT is a cold-stimulated thermogenic tissue found in human infants and hibernating mammals. In newborn humans, up to 5% of total body weight is BAT, however, BAT activity and size decreases with age. Whether BAT plays an important metabolic role in adulthood remains controversial (Kajimura and Saito, 2014; Rogers, 2015). BAT is comprised of adipocytes with small multilocular lipid droplets (LD) and is highly oxidative due to increased mitochondrial content and the expression of uncoupling protein-(UCP) -1. In non-shivering thermogenesis, UCP-1 uses energy to produce heat rather than ATP, by uncoupling mitochondrial oxidative phosphorylation from ATP synthesis. BAT transplantation in mouse models of diet-induced or genetic obesity enhances whole-body metabolism, therefore making BAT is an attractive therapeutic target for obesity treatment in humans (Liu et al., 2015).

In humans, WAT accounts for 3% (extremely lean) to 70% (morbidly-obese) of total body weight (Parlee et al., 2014). WAT is comprised of adipocytes with unilocular LDs (50-70% of AT mass), and cells from the stromal vascular fraction (SVF): preadipocytes (20-40% of AT mass), immune cells (macrophages, T-cell, B-cells), pericytes, endothelial cells and cells of vascular and nerve tissue (Hauner, 2005). The current study focuses on WAT.

Preadipocyte: from commitment to differentiation

Preadipocytes are stromal vascular fibroblasts with adipogenic potential. These cells are proliferative and visually distinguishable from adipocytes by the absence of lipid droplets. Molecular characterization studies in mice have identified these cells as Lin^{-} /$Sca1^{+}$/$CD24^{+}$/$CD29^{+}$/$CD34^{+}$ (Berry and Rodeheffer, 2013). In this study, both $CD24^{+}$ and $CD24^{-}$ populations could differentiate *in vitro*, however *in vivo*, only $CD24^{+}$ cells could reconstitute functional WAT pads in lipodystrophic mice. Recent in *vitro* and *in vivo* mouse studies suggest that preadipocytes lose CD24 expression as they become adipocytes and that CD24 upregulation in early stages of differentiation is necessary for mature adipocyte formation(Berry and Rodeheffer, 2013; Smith et al., 2015).

Several studies have attempted to characterize human SVF populations enriched for adipogenic capacity. Although findings remain unclear, one group identified human precursors as $CD34^{+}$/$CD31^{-}$ (Sengenes et al., 2005). In an effort to standardize findings, the International Federation for Adipose Therapeutics and Science (IFATS) and the International Society for Cellular Therapy (ISCT) have proposed specific criteria for defining adipose precursor cells (Bourin et al., 2013). Using these guidelines, Ong et al characterized depot-specific differences in precursors, demonstrating that subcutaneous (SC) and visceral (VS)

adipocyte precursor cells are $CD10^{hi}$ and $CD200^{hi}$, respectively. Furthermore, they found that $CD10^{hi}$ and $CD200^{lo}$ populations exhibited enhanced adipogenic potential (Ong et al., 2014).

Preadipocytes are derived from mesenchymal stem cells (MSCs) located in the adipose stroma. Alternatively, there are studies that suggest minor contributions from circulating hematopoetic stem cells; however, further studies are needed to confirm these results (Crossno et al., 2006; Sera et al., 2009; Tomiyama et al., 2008). MSCs are pluripotent cells that, depending on the specific stimulus, commit to adipocyte, osteocyte, chondrocyte or myocyte lineages. The transition from MSC to the mature adipocyte occurs in two major stages: 1) commitment of the MSCs to the preadipocyte lineage and 2) the maturation of these preadipocytes into adipocytes (terminal differentiation) (Rosen and Spiegelman, 2014).

Lineage commitment

Several factors are involved in adipocyte lineage commitment including cell density, cell shape, bone morphogenetic proteins (BMPs) and Wnt signaling (Otto and Lane, 2005). The BMP-2 and -4, members of the transforming growth factor (TGF) -β family, promote adipocyte-lineage commitment and white adipocyte differentiation. BMPs stimulate the expression adipocyte-lineage specific genes by signalling through several Smad proteins and the p38 kinase pathway (Tang and Lane, 2012). Downstream targets of BMP include several cytoskeleton-remodelling proteins: lysyl oxidase (Lox), translationally controlled tumor protein 1 (Tpt1) and αB crystallin (Huang et al., 2011).

The C3H10T1/2 clonal cell line was established in 1973, from day 14-17 C3H mouse embryos (Reznikoff et al., 1973). In culture, these uncommitted pluripotent cells are functionally similar to MSCs, and thus act as a valuable model system for characterizing

lineage commitment (Tang et al., 2004). Knockdown of Lox, Tpt1 and αB crystallin in the C3H10T1/2 cells prevents adipocyte lineage commitment (Huang et al., 2011).

The Wnts are secreted glycoproteins that activate adipocyte lineage commitment while inhibiting terminal differentiation (Bowers and Lane, 2008). In their canonical pathway, Wnt ligands signal through the frizzled receptor, resulting in accumulation of β-catenin in the nucleus. This triggers the activation of leukocyte early factor (Lef)-1 and T-cell factor (Tcf) which themselves activate cell cycle proteins c-myc and cyclin D1. It is hypothesized that these events increase the number of cells that commit to the adipocyte lineage (Tang and Lane, 2012). Conversely, ligands such as Wnt10b inhibit terminal differentiation. Wnt6, Wnt10a and Wnt10b levels are decreased during differentiation and their forced expression in 3T3-L1 preadipocytes inhibits differentiation by supressing expression of peroxisome proliferator-activated receptor (PPAR) γ and CCATT-enhancer-binding protein (C/EBP) α (Cawthorn et al., 2012).

Mitotic clonal expansion

The 3T3-L1 clonal cell line was established from 17-19 day old Swiss 3T3 mouse embryos and is widely used to study adipocyte function and development *in vitro* (Green and Kehinde, 1975). The 3T3-L1 cells are fibroblast-like, and are capable of differentiation and lipid accumulation with appropriate adipogenic stimuli. Contrary to human preadipocytes cultured *in vitro*, 3T3-L1 cells require one to two rounds of post-confluence cellular division prior to terminal differentiation (Entenmann and Hauner, 1996). This process, referred to as mitotic clonal expansion (MCE), involves a series of signalling cascades with cell-cycle regulators such as Retinoblastoma (Rb) protein and E2F, and ends with cells in growth arrest

(Skurk and Hauner, 2012; Tang et al., 2003). The chromatin remodelling and DNA unwinding that occur during MCE are believed to facilitate differentiation by enabling interactions between transcription factors and regulatory regions of adipocyte-specific genes (Farmer, 2006).

Terminal differentiation

Growth-arrested preadipocytes can be stimulated to terminally differentiate using an adipogenic cocktail containing insulin, 3-isobutyl-1-methylxanthine (IBMX), dexamethasone and fetal bovine serum (FBS). Early stages of terminal differentiation occur following induction of C/EBPβ and C/EBPδ. This stage is marked by alterations in the preadipocyte cytoskeleton. During this stage, the extracellular matrix (ECM) gradually shifts from a fibronection-rich to laminar environment (Aratani and Kitagawa, 1988). As a result of these structural changes, preadipocyte morphology shifts from fibroblast-like to spherical and adipocyte-like (Ji et al., 2014).

Together, C/EBPβ and δ activate PPARγ and C/EBPα, the master regulators of adipogenesis. Activation of these regulators is sufficient for maintaining differentiation. PPARγ and C/EBPα act synergistically in a positive feedback loop and the promoter of C/EBPα contains a C/EBP regulatory element, which enables its auto-activation. PPARγ is required for differentiation both *in vitro* and *in vivo*, where in its ligand-bound state, PPARγ heterodimerizes with the retinoid X receptor (RXR) (Rosen et al., 1999). The PPARγ-RXR heterodimer binds to nuclear peroxisome proliferator hormone response elements (PPRE) to increase the transcription of genes involved in adipogenesis, glucose homeostasis and lipid catabolism (Grygiel-Gorniak, 2014).

In late stages of terminal differentiation, the multiple small LD within the cell coalesce into one large LD and cells begin expressing metabolic genes and adipokines associated with the adipocyte phenotype (Cristancho and Lazar, 2011). Examples of genes expressed include, fatty acid synthase (FAS), acetyl-CoA carboxylase (ACC), and fatty acid binding protein 4 (FABP4 or aP2) (Spiegelman et al., 1993). With the expression of glucose transporter type (GLUT) -4 during differentiation, adipocytes develop insulin-sensitive glucose transport. Expression of GLUT-1, which is responsible for basal glucose uptake in the undifferentiated state, substantially decreases with differentiation (Hauner et al., 1998).

Adipocyte function: lipid metabolism

Hormonal signals drive lipogenesis and lipolysis in the adipocyte. Lipogenesis describes the process in which energy is used to synthesize of triglyceride (TG). Insulin is a major driver of lipogenesis and induces expression of lipogenic enzymes through sterol regulatory element binding protein (SREBP) -1 (Proenca et al., 2014). Lipogenesis occurs either by 1) uptake and re-esterification of NEFA to a glycerol-3-phosphate (G3P) or by 2) *de novo* lipogenesis (DNL), a process that involves the synthesis of fatty acids from non-lipid substrates such as carbohydrates (Gathercole et al., 2011; Roberts et al., 2009).

The glycerol backbone of TG is generated via the glycolytic pathway, which converts glucose into G3P. Alternatively, glyceroneogenesis generates G3P using non-glucose precursors (e.g. pyruvate); a process catalyzed by phosphoenolpyruvate carboxykinase (PEPCK). In fasting and high sucrose-fed rats, Nye et al found that glyceroneogenesis was the predominant source of G3P in AT (Nye et al., 2008).

The adipocyte acquires the fatty acid component of TG from hepatic sources, dietary sources (via lipoprotein delivery) or is generated via DNL by the adipocyte. In DNL, the conversion of acetyl-CoA by ACC and FAS generates palmitate, which can be further elongated and desaturated (Gathercole et al., 2013). Although AT DNL is believed to contribute minimally to whole body adiposity in humans, growing evidence suggests that its activation improves systemic insulin sensitivity and glucose homeostasis (Gathercole et al., 2013; Rosen and Spiegelman, 2014).

Lipolysis describes the breakdown of TG to release NEFA that occurs when energy is required. Three enzymes account for over 90% of the lipolytic activity in the adipocyte: adipose triglyceride lipase (ATGL), hormone sensitive lipase (HSL), and monoglyceride lipase (MGL) (Young and Zechner, 2013). Together, these enzymes catalyze the hydrolysis of TG into diglyceride (DG) and monoglyceride (MG).

ATGL and HSL are the rate-limiting enzymes of lipolysis and catalyze the hydrolysis of TG to DG and DG to MG, respectively. ATGL is activated by α/β hydrolase fold domain 5 (Abhd5) and inhibited by a G0/G1 switch gene 2 (G0S2) protein, whereas HSL is activated by cyclic adenosine monophosphate (cAMP)-dependent Protein Kinase A (PKA) (Fruhbeck et al., 2014). PKA also regulates lipolysis by hyperphosphorylating the LD perilipin coat. Hyperphosphorylation of perilipin induces conformational changes that enable hydrolysis of TG within the LD by facilitating lipase access. Lastly, in the final step of TG breakdown, MGL catalyzes the hydrolysis of MG to liberate the NEFA and glycerol moieties (Rosen and Spiegelman, 2014).

Insulin is the major suppressor of lipolysis, and this is accomplished through both Akt -dependent and -independent mechanisms. In the Akt-dependent pathway, Akt activates

phosphodiesterase-3b (PDE-3b) by Ser^{273} phosphorylation. Activated PDE-3b reduces cAMP levels, thereby inhibiting PKA activity (Choi et al., 2010). The same authors proposed an alternative Akt-independent, PI3K-dependent mechanism wherein PKA phosphorylation of perillipin-1 is specifically blocked.

Secretory and immune function of adipose tissue

AT mediates its role as an active endocrine organ through the secretion of small signaling peptides (adipokines), enabling cross-talk with other organs such as the muscle, liver and brain. Leptin, the first adipokine to be discovered, binds to leptin receptors in arcuate nucleus of the hypothalamus and, in turn, regulates body weight through the promotion of satiety and increased energy expenditure (Khan and Joseph, 2014; Zhang et al., 1994). Another adipokine, adiponectin, improves insulin sensitivity in liver and also enhances glucose uptake and fatty acid oxidation in muscle (Karbowska and Kochan, 2006).

AT also performs an immune-modulatory function through the secretion of anti- (e.g. adiponectin) and pro- (e.g. TNF-α, IL-1β and IL-6) inflammatory adipokines. The secretion of pro-inflammatory adipokines within AT further exacerbates inflammation and insulin resistance by increasing recruitment of circulating $Ly6C^{hi}$ pro-inflammatory monocytes and by activating the M1 pro-inflammatory phenotype of the AT-resident macrophages (ATM) (Kraakman et al., 2014). Conversely, the M2 phenotype, which is activated by anti-inflammatory cytokines such as IL-10, maintains AT homeostasis by promoting tissue repair, cell proliferation and attenuating inflammatory responses (Mills, 2012). ATM secreted factors also impact cellular function. In human and 3T3-L1 preadipocytes, incubation with

ATM secreted factors can block differentiation and proliferation (Constant et al., 2006; Lacasa et al., 2007).

White adipose tissue depots

The main WAT depots in humans are subcutaneous and visceral AT (SAT and VAT, respectively). Approximately 80% of all body fat is stored as SAT (Ibrahim, 2010). VAT consists of deep fat depots surrounding vital organs. VAT constitutes 10-20% and 5-8% of total fat mass in males and females, respectively (Lee et al., 2013).

Compared to SAT, VAT is more lipolytic when stimulated with adrenergic agonists and its accumulation is a greater predictor of metabolic dysfunction (Lee et al., 2013). In addition, VAT production of pro-inflammatory cytokines is greater and preadipocytes from this depot are more susceptible to apoptotic stimuli (Lee et al., 2013; Tchkonia et al., 2005). Although not as metabolically active as VAT, SAT also contributes to metabolic dysfunction through the secretion of pro-inflammatory cytokines (Silva et al., 2015). Furthermore, if SAT storage capacity is exceeded, the subsequent ectopic lipid deposition and lipotoxicity also promotes metabolic dysfunction.

SAT adipocytes are smaller, more insulin sensitive and are better able to store lipid than their VAT counterparts (Hauner et al., 1988; Ibrahim, 2010). In general, the number of preadipocytes and their differentiation capacity is greater in SAT than VAT (Lessard et al., 2014). Regional variations between VAT and SAT may stem from differences in preadipocyte populations. Two subtypes of preadipocytes can be distinguished in humans, with SAT containing the subtype that is more replicative, adipogenic and resistant to tumor necrosis factor (TNF) -α induced apoptosis (Tchkonia et al., 2005). Supporting the

hypothesis of VAT and SAT-specific populations, Gesta el al observed depot-specific differential expression of preadipocyte and adipocyte developmental genes. In humans, several of these genes exhibited changes in expression that closely correlated with the pattern of fat distribution (Gesta et al., 2006).

Adipose tissue expansion and obesity: hyperplasia and hypertrophy

Obesity is defined as abnormal or excess AT accumulation resulting in a body-mass index (BMI; a calculation of an individual's weight relative to their height) that exceeds 30 kilograms (kg)/meter (m) ^{2}. Obesity is associated with insulin resistance, cardiovascular disease and type 2 diabetes (T2D) (WHO, 2015). Obesity is marked by chronic low-grade inflammation stemming from increased secretion of pro-inflammatory cytokines and circulating NEFA.

AT expands by both hyperplasia and hypertrophy. Interestingly, 10-25% of obese individuals are metabolically healthy, which may be linked to hyperplastic (increase in cell number) versus hypertrophic (increase in cell size) AT expansion (Bluher, 2010). When AT expansion is hyperplastic, adipocytes are more numerous, but are normal-sized and metabolically neutral, and inflammatory macrophage accumulation does not occur (Ahima and Lazar, 2013; Sun et al., 2011). Weight gain through hyperplastic expansion is associated with the metabolically healthy but obese (MHO) phenotype; wherein energy is evenly distributed and each cell remains functionally responsive. Adipocyte hypertrophy is associated with inflammatory immune cell/macrophage infiltration, increased lipolysis and insulin resistance, raising the risk for atherosclerosis and T2D. Low generation of adipocytes is linked to hypertrophy and as such, the etiology of obesity is dependent on both the

differentiation capacity of the preadipocytes and their abundance within the AT (Arner et al., 2010).

Using HFD-fed mice, Jeffery et al observed that VAT responds to over-nutrition with both hyperplastic and hypertrophic expansion, whereas SAT does so mainly through hypertrophy. Furthermore, they found that functional phosphoinositide 3-kinase (PI3K)-Akt2 signaling was required for this AT expansion (Jeffery et al., 2015). In a separate study using HFD-fed mice, Strissel et al detailed the temporal dynamics of AT development. In early stages, hypertrophic expansion predominated with little change in adipocyte number. At week 16, they observed high levels of cell death (~80% adipocyte cell death) and increased macrophage infiltration. Finally at week 20, they observed a reduction in adipocyte cell death (~16%) accompanied by a significant increase of smaller adipocytes (Strissel et al., 2007).

There is also evidence of differences in expansion in humans between the different AT depots. In healthy normal-weight adults, Tchoukalova et al detailed human AT expansion following 8 weeks of over-feeding. In this study, over-feeding resulted in hyperplastic versus hypertrophic expansion in lower body versus upper SAT depots, respectively (Tchoukalova et al., 2010).

By comparing the incorporation of ^{14}C stable-isotopes (derived from above-ground nuclear bomb tests during the Cold War, 1955 to 1963) into genomic DNA of human children, adolescents and adults, Spalding et al established that total adipocyte number increases throughout childhood and levels off in adulthood, with obese individuals reaching a higher plateau than lean individuals (Spalding et al., 2008). Furthermore they found that ~10% of adipocytes turn-over annually in adulthood, irrespective of BMI. In a follow-up to

this study, Arner et al reported that individuals with hypertrophic AT generated 70% less adipocytes per year compared to individuals with hyperplastic AT (Arner et al., 2010).

The preadipocyte pool and adipose tissue dysfunction

Dysfunctional SAT is associated with lipotoxicity, ectopic lipid accumulation and enlarged VAT (Tchkonia et al., 2013). The spill-over hypothesis proposes that when hypertrophied SAT adipocytes reach their maximal expansion limit, excess lipid is deposited first in VAT and then ectopically, in non-AT such as liver or muscle (O'Connell et al., 2010). Thus, SAT is believed to act as a buffer, protecting other tissues from post-prandial fluxes of circulating NEFA (Frayn, 2002).

Several studies provide evidence for this protective role of SAT. In humans, Snijder et al observed that increased thigh SAT correlates with favourable glucose and lipid levels (Snijder et al., 2005). With HFD mice, Lu et al demonstrated that increasing SAT volume through hyperplasia resulted in a reduction in liver steatosis, improved glucose tolerance and insulin sensitivity (Lu et al., 2014).

Preadipocyte recruitment, self-renewal and adipogenic potential are important for hyperplastic AT expansion. Consistent with this concept, several studies have reported reduced numbers of adipocyte precursors in human obesity (Onate et al., 2012; Tchoukalova et al., 2007). Using a stable isotope approach to measure adipogenesis in mice, Kim et al observed that SC adipocyte turnover inversely correlates with insulin sensitivity in obesity (Kim et al., 2014). Furthermore, they postulated that differentiation without a preceding cell division step results in preadipocyte pool exhaustion, thus limiting SAT expansion.

Adipose tissue and insulin signalling

Following the digestion of a meal, glucose is absorbed and enters the circulation. As blood glucose concentration begins to rise, it stimulates the secretion of insulin by the pancreatic β-cells. Insulin is a polypeptide dimer comprised of an A chain (21 residues) and B chain (30 residues) linked by three disulfide bridges (Hua, 2010). In AT, insulin promotes adipogenesis, glucose uptake and lipogenesis, while suppressing lipolysis (Samuel and Shulman, 2012). The IR is expressed in most tissues, with higher levels found in the classical target tissues (i.e. liver, muscle and AT) (Golan and Tashjian, 2012).

Insulin signaling in adipose tissue: the Akt pathway

Insulin receptor activation through insulin binding results in auto-phosphorylation of its tyrosine kinase domains and the subsequent tyrosine (Tyr) phosphorylation of intracellular insulin receptor substrate (IRS). Tyr-phosphorylated IRS serves as a docking site for the Src-homology (Sh)-2 domain of PI3K. PI3K generates 3-phosphorylated phosphoinositides and these lipids attract phosphoinositide-dependent kinase-1 (PDK-1) and Akt, resulting in the phosphorylation of Akt at Threonine (Thr) ^{308} by PDK-1. The mammalian target of rapamycin complex (mTORC) -2 fully activates Akt by a second phosphorylation event at Serine (Ser) ^{473} (Tsuchiya et al., 2013). In the adipocyte, Akt regulates insulin-stimulated glucose transport, via GLUT4 translocation to the plasma membrane. In the preadipocyte, insulin signaling is not coupled to glucose transport, but rather linked to adipogenic responses (Hauner et al., 1998).

Inhibition of the anti-adipogenic Forkhead transcription factor (FoxO1) by insulin occurs through Akt-dependent phosphorylation (Farmer, 2006). When FoxO1 is active, it translocates to the nucleus where it promotes gluconeogenesis, lipolysis, and lipogenesis (Fan et al., 2009). The mechanism by which FoxO1 inhibits adipogenesis is not fully understood. One group reported that FoxO1 binds to promoter sites of PPARγ, preventing PPARγ expression (Armoni et al., 2006). Furthermore, through direct binding with PPARγ, FoxO1 also acts as a trans-repressor of PPARγ. FoxO1-bound PPARγ is unable to interact with its cognate enhancer element and activity is thus supressed (Fan et al., 2009). With insulin stimulation, FoxO1 is phosphorylated by Akt, and thus unable to translocate into the nucleus to suppress adipogenic gene expression.

Insulin also stimulates expression of SREBP-1, a key transcription factor (Farmer, 2006). SREBP-1 binds to sterol regulatory elements (SRE) in promoter regions of genes involved in sterol biosynthesis and fatty acid synthesis, thereby promoting their transcription (Shimano, 2001). SREBP-1 also promotes adipogenesis through the activation of PPARγ and this occurs through the binding of SREBP-1 to an E-box motif located in the PPARγ promoter (Fajas et al., 1999). SREBP-1 also activates PPARγ by promoting the expression and secretion of endogenous PPARγ ligands (Kim et al., 1998).

Protein tyrosine kinases: insulin receptor and insulin receptor substrate

Insulin signals through several closely related receptors; the IR, the insulin-like growth factor 1 receptor (IGF1R) or through IGF1R-IR hybrid receptors. Hybridization is facilitated as the IR and IGF1R share from 41% to 84% structural homology (depending on the domain), however, insulin binds them with lower affinity (De Meyts et al., 2000; Slaaby,

2015). Alternatively, insulin-like growth factors (IGFs) stimulate signaling through the IR, however, they do so with 10 to 100 fold lower affinity than insulin (Blakesley et al., 1996).

The IR is a $(\alpha\beta)_2$ transmembrane homodimer with intrinsic tyrosine kinase activity. Alternative splicing of IR mRNA yields two isoforms, IR-A and IR-B. The IR-A, the truncated isoform lacking 12 residues near the C-terminus of the α-subunit, is expressed ubiquitously, whereas IR-B expression is localized to insulin target tissues (Belfiore et al., 2009). IR-A binds insulin with greater affinity than IR-B, and is the predominating isoform found in human SC preadipocytes (Back and Arnqvist, 2009). These authors also report that following differentiation of human SC preadipocytes, total expression of the IR increases more than 10-fold relative to the IGF1R, with IGF1R levels remaining constant.

Activated IR interacts with proteins containing Sh2 or phosphotyrosine-binding (PTB) domains. The IRS proteins contain an N-terminal Pleckstrin Homology (PH) domain followed by a PTB domain and a variable length C-terminal containing multiple Tyr phosphorylation sites. The PTB of IRS binds directly to phosphorylated Tyr^{960} within the NPXY motif of the IR-β subunit, whereas the PH domain binds to cell membrane 3-phosphorylated phosphatidylinositol lipids (Ramalingam et al., 2013; Wagner et al., 2013). The PH domain may facilitate the IR interaction by promoting membrane localization of IRS-1 (Vainshtein et al., 2001). Finally, the Tyr residues in the C-terminal region, when appropriately phosphorylated, act as binding sites for specific downstream Sh2 domain-containing signaling proteins. IRS-1 and IRS-2 are the main isoforms found in humans, with the former predominating in AT and muscle, and the latter in liver. IRS proteins play a crucial role in adipogenesis since, *in vivo,* IRS-$1^{-/-}$ IRS-$2^{-/-}$ double knockout mice display

severe reduction of WAT and *in vitro* these cells are unable to differentiate (Miki et al., 2001).

Regulation of insulin signaling: a balance of phosphorylation

The status of Tyr phosphorylation of IR and IRS proteins is determined by the activities of protein tyrosine phosphatases (PTPs) and kinases (PTKs). The Tyr phosphorylation facilitates specific interactions with downstream proteins by acting as Sh2 binding sites. IRS1 contains approximately 20 Tyr sites at its C-terminal domain (Boura-Halfon and Zick, 2009). The role of PTPs in insulin signaling is complex and several PTPs including PTP-BL, PTP-RQ and leukocyte common antigen–related (LAR) and PTP-1B are implicated in adipogenesis (Bae et al., 2012; Gurzov et al., 2015). PTP-1B, encoded by the *PTN1* gene, is the most extensively studied PTP in humans. Polymorphisms in *PTN1* are linked with increased risk insulin resistance, T2D and obesity in humans (Tsou and Bence, 2012).

Insulin signaling is also modulated through Ser/Thr residue phosphorylation of IRS via Ser/Thr Kinases. IRS-1 contains more than 50 Ser/Thr sites and depending on the specific residue, phosphorylation can either promote or inhibit transduction of the signal (Copps and White, 2012). For example, residues adjacent to Tyr residues can inhibit signaling by interfering with the SH2 domain interactions. Alternatively, insulin-stimulated activation of Akt positively regulates signaling via Ser phosphorylation of the IRS PTB domain. This Ser phosphorylation protects against PTP-mediated Tyr dephosphorylation at the PTB domain, allowing IRS to maintain its active conformation (Paz et al., 1999). Finally, several known inducers of insulin resistance (e.g. TNF-α and NEFA) also stimulate Ser/Thr kinases (Boura-Halfon and Zick, 2009). Activity of these kinases is also regulated in part by Ser/Thr

phosphatases. Examples of these include Protein Phosphatase (PP)-1, PP-2A, and PH-domain-and-Leucine-rich-repeat Protein Phosphatases (PHLPPs) (Xu et al., 2014).

Mutational analysis reveals human (h) Ser^{312}, or mouse (m) Ser^{307} on IRS-1, as a major target of phosphorylation by c-Jun N-terminal kinases (JNK). Due to their proximity to the IRS PTB domain, phosphorylation of $hSer^{312}$ and other neighboring Ser/Thr residues are believed to sterically disrupt interaction between the activated IR and IRS (Copps and White, 2012; Du and Wei, 2014). Phosphorylation of this residue is linked to a variety of metabolic dysfunctions including hyperinsulinemia, T2D and obesity (Hancer et al., 2014). Using human SC adipocytes, Danielsson et al observed that phosphorylation at this residue required chronic stimulation with high concentrations of insulin (Danielsson et al., 2006). The early stages of T2D are marked by chronic hyperinsulinemia, therefore, the authors postulated that $hSer^{312}$ phosphorylation may occur during this stage, thus further exacerbating the insulin resistant state.

Nutrient stress and adipose tissue

Recent studies suggest that nutrient stress in obesity and T2D causes "metabolic" inflammation and insulin resistance in insulin-target tissues (Odegaard and Chawla, 2013). Obesity is a major risk factor for T2D, a disease characterized by insulin resistance in target tissues. Early stages of T2D are marked by chronic hyperinsulinemia, wherein the β-cells compensate for decreased insulin sensitivity in order to maintain euglycemia (Martyn et al., 2008). The following sections describe cell culture models of type 2 diabetes, based on hyperglycemia and chronic hyperinsulinemia to induce insulin resistance.

General mechanisms of hyperglycemia-mediated insulin resistance

At supraphysiological levels, glucose impairs AT insulin sensitivity, however, this process is incompletely understood. Hyperglycemia produces advanced glycation end products (AGEs) that may inhibit insulin signaling via methylglyoxal binding to IRS-1, and the impairment of IRS Tyr phosphorylation (Liu et al., 2013; Riboulet-Chavey et al., 2006). Alternatively, hyperglycemia increases flux into hexosamine-synthesis pathway (Teo et al., 2010). Induction of the hexosamine pathway promotes the O-GlcNAcylation of IRS proteins and IR, thus inhibiting their interactions and preventing the latter from dimerizing (Boucher et al., 2014).

Chronic hyperglycemia also induces DG synthesis, activating protein kinase C (PKC) (Filippis et al., 1997; Hoffman et al., 1991). PKC activation is also thought to occur through the hyperglycemia-induced production of reactive oxygen species (ROS) (Haber et al., 2003). Activated PKC inhibits IR Tyr kinase activity through Ser phosphorylation (without impairment of insulin binding), attenuates IRS-1 Tyr phosphorylation by activating specific PTPs and promotes IRS-1 Ser/Thr phosphorylation (Bollag et al., 1986; Mussig et al., 2005). In skeletal muscle hyperglycemia promotes the formation of a receptor of AGE/IRS-1/Src complex that activates PKC-α (Cassese et al., 2008). PKC-α mediates impairment of insulin signaling by phosphorylating IRS-1 at $mSer^{307}$ (Boucher et al., 2014).

General mechanisms of hyperinsulinemia-mediated insulin resistance

Hyperinsulinemia is traditionally viewed as a consequence of insulin resistance in HFD-induced obesity, however, recent rodent studies suggest that it may play a causal role

(Mehran et al., 2012). Furthermore, transgenic mice overexpressing insulin and humans with insulinomas, display reduced insulin responses (Catalano et al., 2014). Consistent with these findings, isolated rat adipocytes exposed to hyperinsulinemia for 2 or 4 hours display dose-dependent losses of IRs and marked post-receptor defects in glucose transport (Marshall and Olefsky, 1980). Both *in vitro* and *in vivo*, prolonged exposure to insulin decreases IR numbers, which subsequently impairs insulin sensitivity (Gavin et al., 1974). Hyperinsulinemia also drives AT inflammation in obese mice, possibly through increased macrophage expansion and pro-inflammatory gene expression, and this contributes to suppression of insulin-stimulated adipocyte DNL and to systemic insulin resistance (Pedersen et al., 2015).

Chronic hyperinsulinemia causes impairment at both the IR and post-receptor signaling. Prolonged exposure to insulin activates IRS-1 ubiquitin-proteasome degradation, a process that is IR-mediated (Zhande et al., 2002). Recently, using Förster Resonance Emission Transfer (FRET) with Chinese Hamster Ovary (CHO) cells, Catalano et al observed that the Tyr Kinase domain of the IR is structurally altered and exhibits decreased autophosphorylation with prolonged hyperinsulinemia (Catalano et al., 2014). This decrease in IR Tyr phosphorylation was independent of IR amount and membrane localization of the receptor.

The effects of chronic high glucose on adipocytes *in vitro*

High glucose (≥15 mM glucose) is used to inhibit insulin-stimulated responses in several *in vitro* models of insulin resistance. Burén et al found that rat adipocytes isolated from epididymal fat pads and pre-incubated with 25 mM glucose for 24 hours exhibit lower

insulin-stimulated glucose uptake in comparison to 5 mM treatments (Buren et al., 2003). Furthermore, this effect has also been observed in 3T3-L1 adipocytes treated with 25 mM glucose for 48 hours (Gao et al., 2010).

The effects of high glucose on the adipocyte extend to the cellular stress and inflammatory responses. Thioredoxin interacting proten (Txnip) modulates insulin sensitivity by altering phosphatase and tensin homolog (PTEN) activity, the latter being an enzyme that targets 3-phosphorylated phosphoinositides. With 48 hour high glucose treatment, Txnip is enhanced in human AT, and this in turn increases transcription of pro-inflammatory IL-1β promoting an insulin resistant state (Koenen et al., 2011). Furthermore, in primary cultured human adipocytes, 24 hour treatment with 25 mM glucose results in the induction of endoplasmic reticulum (ER) stress and, unexpectedly, in increased levels of Ser^{473} Akt phosphorylation (Alhusaini et al., 2010).

The effects of chronic insulin and high glucose on adipocytes *in vitro*

Despite the aforementioned findings, several studies with 3T3-L1 adipocytes suggest that high glucose alone is not sufficient in fully generating insulin resistant cells (Ling et al., 2012; Robinson et al., 2014). Instead, these studies combine insulin with high glucose, which act synergistically to generate an insulin resistant state. Chronic exposure of 3T3-L1 adipocytes to the combination results in decreased insulin-stimulated glucose uptake and impaired insulin signaling downstream of PI3K (Greene et al., 2001; Ling et al., 2012; Nelson et al., 2000; Robinson et al., 2014; Ross et al., 2000). Moreover, Renström et al found that pre-incubation of isolated human adipocytes with 20 mM glucose for 24 hours resulted

only in a minor decrease of insulin-stimulated glucose uptake, and this effect was amplified with co-treatment with 10^4 μU/mL insulin (Renstrom et al., 2007).

The effects of high glucose on adipocyte differentiation *in vitro*

Differentiation of 3T3-L1 preadipocytes in high glucose generates hypertrophic adipocytes that express more monocyte chemoattractant protein-1 (MCP-1), a factor that mediates macrophage recruitment (Han et al., 2007). Consistent with a pro-inflammatory phenotype, these hypertrophic adipocytes display increased NF-κB and decreased PPARγ activity. A separate study found that differentiation was enhanced in normal glucose conditions when compared to the high glucose conditions, as measured by Oil Red O staining of neutral lipid and by quantification of cellular triglyceride mass (Gagnon and Sorisky, 1998). Differentiation in high glucose has also been reported to increase ROS production and decrease insulin-stimulated glucose uptake in the mature adipocytes (Lin et al., 2005). Finally, high glucose differentiation of 3T3-L1 cells has recently been linked with increased mitochondrial and ER stress (Tanis et al., 2015).

The effects of chronic insulin and high glucose on human preadipocytes *in vitro*

To our knowledge, the combinatorial effects of chronic insulin and high glucose on the human preadipocyte has yet to be explored. In a study using human preadipocytes, Moreno-Navarrete et al found that 48 hour pre-incubation with 100 mM glucose followed by acute 100 nM insulin stimulation for 10 minutes led to a significant decrease in Ser^{473} pAkt levels when compared to cells pre-incubated with 17.5 mM glucose (Moreno-Navarrete et al., 2013). It should be noted that 100 mM glucose is extremely high and it is an unusual

concentration to use in cell culture studies. Finally, confluent 3T3-L1 preadipocytes exposed to 25 mM glucose and acutely stimulated with 100 nM insulin, display decreased levels of insulin-stimulated IRS-1 Tyr phosphorylation and decreased insulin-stimulated IRS-1-PI3K association (Gagnon and Sorisky, 1998).

Cell model: human primary preadipocytes

The present study uses human primary preadipocytes, enabling a representative characterization of the effects of nutrient stress on human AT development and function *in vitro*. This model provides added accuracy as it rules out species-specific differences that accompany the murine 3T3-L1 cell lines. However, there are also limitations to this model, which include variability in cellular responses amongst patients, introduced by donor heterogeneity (e.g. age, sex, BMI), and the limited preadipocyte passage number in culture (3-4 passages, after which they lose the ability to differentiate).

Rationale

The manner in which AT expands influences metabolic health; hyperplastic expansion is protective, whereas hypertrophic expansion is linked to inflammation, insulin resistance, and metabolic dysfunction. The polarization of hyperplasia versus hypertrophy is dependent on the adipogenic responses and size of the preadipocyte pool. Despite this, very few studies have examined the effects of high glucose-based nutrient stress on the preadipocyte. Studies using 3T3-L1 adipocytes demonstrate *in vitro* generated insulin resistance following chronic pre-incubation in insulin and high glucose (Nelson et al., 2000;

Robinson et al., 2014). Thus, we investigated whether these same conditions could generate insulin resistance and impair insulin-stimulated adipogenesis in the human preadipocyte. Detailing the effects of glucotoxicity at the level of the preadipocyte may elucidate mechanisms by which dysfunctional versus healthy human AT remodelling and expansion occurs *in vivo*.

Hypothesis

Chronic exposure to insulin and/or high glucose causes insulin resistance in human preadipocytes.

Objectives

Objective 1: Determine the conditions in which insulin and/or high glucose inhibits insulin signaling in human preadipocytes

Objective 2: Characterize the effect of insulin and/or high glucose on preadipocyte pro-inflammatory adipokine expression

Objective 3: Characterize the effect of insulin and/or high glucose on adipocyte differentiation

METHODOLOGY

Isolation and culture of human preadipocytes

Human SC abdominal AT was obtained from 6 female patients undergoing elective abdominal surgery (approved by Ottawa Health Science Network Research Ethics Board). Mean age was 57±6 years, and mean BMI was 27±4 kg/m^2 (±SD). AT was carried to the laboratory in DMEM (Dulbecco's modified Eagle's medium):F12 (1:1) supplemented with 33 mM biotin, 17 μM calcium pantothenate, 200 U/ml penicillin, 0.2 mg/ml streptomycin and 100 U/ml nystatin. Next, AT was dissected to remove blood vessels and connective tissue. The dissected tissue was incubated (60 minutes, 37°C) with collagenase CLS type I (200 U/g tissue, Worthington, Lakewood, NJ) in DMEM:F12 supplemented with 33 μM biotin, 17 μM calcium pantothenate, 100 U/ml penicillin, 0.1 mg/ml streptomycin and 50 U/mL nystatin on a rotating mixer. The digested tissue was filtered using 200 μm nylon filter and subsequently centrifuged (180 x g, 20 minutes) to separate the SVF from mature adipocytes. Cells were further processed through progressive size filtration using 100, 50 and then 25 μM nylon filters. Filtrates were centrifuged (180 x g, 20 minutes) and the resulting pellet incubated for 5 minutes in red blood cell lysis buffer (155 mM NH_4Cl, 5.7 mM K_2HPO_4, 0.1 mM EDTA; pH 7.3). Following red blood cell lysis, cells were plated in DMEM (5 mM glucose) supplemented with 10% FBS, 100 U/ml penicillin, 0.1 mg/ml streptomycin and 50 U/ml nystatin (referred to henceforth as growth media) and grown until confluence. Cells were either passaged and expanded directly for experiments or cryopreserved for future use.

Nutrient Stress: pre-treatment of human preadipocytes

Confluent preadipocytes were placed under nutrient stress conditions for 48 hours (5 mM or 25 mM glucose with 0.6 nM insulin or 0.01 N HCl vehicle control, in DMEM supplemented with 100 U/ml penicillin, 0.1 mg/ml streptomycin and 1% calf serum). Insulin signaling experiments (Objective 1) and pro-inflammatory cytokine expression experiments (Objective 2) were performed immediately following the 48 hour nutrient stress.

Acute stimulation of insulin signaling

Preadipocytes were grown until confluence in 35 mm plates seeded at a density of $3x10^4$ cells/cm^2. Immediately following the 48 hour nutrient stress treatment, preadipocytes were rinsed with glucose adjusted DMEM, then incubated in assay buffer (5 mM or 25 mM glucose DMEM supplemented with 100 U/ml penicillin, 0.1 mg/ml streptomycin and 1% calf serum) with 100 nM insulin or 0.01 N HCl vehicle for 5 or 15 minutes. The medium was then removed, cells were rinsed with ice cold 1x phosphate-buffered saline (PBS), and proteins were solubilized in Laemmli buffer supplemented with 5% β-mercaptoethanol, 1 mM sodium orthovanadate (Na_3VO_4), 5 mM pH 8 EGTA, 50 mM sodium fluoride (NaF), and 5 mM sodium pyrophosphate (NaPPi); referred to henceforth as Laemmli buffer with phosphatase inhibitors (Laemmli, 1970).

Lowry assay

For Laemmli-solubilized proteins, protein quantification was performed using a Lowry assay, with bovine serum albumin (BSA) as a standard. Samples were prepared in

triplicate, using 2-5 µl of lysate adjusted to a final volume of 200 µl with H_2O. First, 20 µl of 1.5 mg/ml deoxycholate (DOC) reagent was added to each diluted sample, vortexed and incubated (10 minutes, room temperature). Next, 20 µl of 72% v/v trichloroacetic acid (TCA) was added. Samples were vortexed and centrifuged (21 000 x g, 10 minutes). Supernatants were discarded and tubes were inverted for 45-60 minutes to allow the protein pellets to air dry. To the protein pellets, 25 µl of reagent A' (mixture of BioRad reagents A and S, Hercules, CA, USA) was added and samples were vortexed and incubated (5 minutes, room temperature). Finally, 200 µl Reagent B was added, samples were vortexed and incubated (15 minutes, room temperature). Samples were transferred to a 96-well microplate and absorbance was read at 750 nm using a FLUOstar Galaxy plate reader (BMG Labtech, Ortenberg, Germany).

Immunoprecipitation

Preadipocytes were grown until confluence in 60 mm plates seeded at a density of $3x10^4$ cells/cm^2. Following 48 hour nutrient stress, media was aspirated, cells were rinsed with ice cold PBS and then lysed in 500 µl ice cold cell lysis buffer (PBS, 1% NP-40, 200 mM Na_3VO_4, 0.1 mg/ml PMSF, 10 mg/ml aprotinin, 10 mg/ml leupeptin, 4 mg/ml benzamidine, 10 mM NaF, 5 mM NaPPi and 1 mM β-glycerophosphate) on ice for 15 minutes. Lysates were transferred into pre-chilled tubes, vortexed and centrifuged (18 000 x g, 10 minutes; 4°C) to pellet nuclei and cell membranes. Supernatants were transferred into new tubes, putting aside 40 µl of each sample for quantification using the bicinchoninic acid (BCA) assay.

Two sets of tubes were prepared and incubated on a nutator for 60 minutes at 4°C. The first set consisted of 500 µl of ice cold cell lysis buffer, 40 µl of washed protein A/sepharose beads and 5 µl of mouse anti-phosphotyrosine antibody (pY20, 1 mg/ml, abcam, Cambridge, MA, USA). In the second set, the cell lysate supernatants were added to 40 µl of washed protein A/sepharose beads. Following the incubation, the first set of tubes was centrifuged (18 000 x g, 1 minute, 4°C) and the supernatants were aspirated. The antibody-linked bead pellets were washed with ice cold cell lysis buffer and incubated (overnight, 4°C) with ~0.16 mg of cleared protein supernatants derived from the second set (quantified via BCA assay). Immunoprecipitated proteins were washed using ice-cold lysis buffer and solubilized in 75 µl of Laemmli buffer containing phosphatase inhibitors. Solubilized proteins were vortexed, boiled for 5 minutes and stored at -20°C until further use. Prior to loading, samples were thawed, vortexed, and centrifuged (21 000 x g, 5 minutes) to pellet the beads.

Bicinchoninic acid assay

For immunoprecipitation experiments, protein quantification was performed using BCA Protein Assay Reagent Kit (Pierce, Rockford, IL, USA), using BSA as a standard. Samples were prepared in triplicates, adding 10 µl of sample to 250 µl of H_2O and adjusting to a final volume of 500 µl using cell lysis buffer. Next, 500 µl of BCA reagent (mixture of 50:48:2, v/v/v) was added to each diluted sample. Samples were vortexed and incubated at 60°C for 1 hour. Samples were cooled to room temperature, transferred to cuvettes and absorbance was read at 562 nm using an Ultrospec 3100 pro-spectrophotometer (GE Healthcare Life Sciences; Baie d'Urfé, QC, CA).

Differentiation of human preadipocytes

For the adipogenesis experiments (Objective 3), preadipocytes were differentiated for 14 days immediately following the 48 hour nutrient stress, maintaining the initial respective glucose concentrations. The differentiation medium was changed every 3-4 days and consisted of: 5 mM or 25 mM glucose growth media supplemented with 0.25 mM IBMX, 100 μM indomethacin, 0.5 μM dexamethasone and 0.85 μM insulin. On day 14, TG was extracted (refer to *Triglyceride extraction and quantification* section) and protein was solubilized using of Laemmli buffer.

Immunoblot analysis

Equal amounts of solubilized protein (5-20 μg) or equal volumes of immunoprecipitated protein (50 μl) were separated using SDS-PAGE (200 V; 60-75 minutes) and transferred to nitrocellulose membranes (70 V; 85-105 minutes). Membranes were incubated in PBS with 3% BSA (immunoprecipitation experiments) or 5% skim milk for 60 minutes to block non-specific binding. Membranes were incubated overnight in the following antibodies directed against: PhosphoAkt Ser^{473} (1:1000; Cell Signaling Technology, Beverly, MA, USA), Akt (1:1000; Cell Signaling Technology,), ERK 1/2 (0.25 μg/ml or 0.125 μg/ml, Millipore, Billericia, MA, USA), IRS-1 (1:1000 or 1:500; Cell Signaling Technology), IR-β (1:1000 or 1:500; Cell Signaling Technology), PPARγ (1:1000; Cell Signaling Technology), FAS (1:1000; Cell Signaling Technology) and SREBP-1c (1:1000; Santa Cruz Biotechnology, Dallas, TX, USA). Next, membranes were incubated in the appropriate horseradish peroxidase-conjugated secondary antibody for 60 minutes and

immunoreactivity was determined using the Immobilon Western chemiluminescence HRP Substrate (Millipore, Billericia, MA, USA). Relative band intensities were quantified using the AlphaEaseFC software (Alpha Innotech, San Leandro, CA) and are expressed as integrated optical density (IOD) units.

RNA extraction and DNAse treatment

Preadipocytes were grown until confluence in 12-well plates seeded at a density of $3x10^4$ cells/cm^2. Immediately following 48 hour nutrient stress, the medium was aspirated and cells were lysed in 1 ml of Qiazol Reagent (Qiagen, Venlo, Limburg, Netherlands). Cell lysates were mixed by inversion for 5 minutes. Next, 200 µl of chloroform was added and the samples were mixed for 15 seconds, then left at rest for 2-3 minutes to allow for phase separation. Samples were centrifuged (12 000 x g, 15 min, 4°C) and the upper aqueous phase was added to 500 µl isopropanol and mixed by inversion for 5 seconds. These samples were incubated (10 minutes, room temperature), centrifuged (12 000 x g, 8 minutes, room temperature), and the RNA pellets were washed in 1 ml of 75% ethanol (v/v), diluted with diethylpyrocarbonate (DEPC)-treated H_2O (centrifuged 7 500 x g for 5 minutes at room temperature after re-suspension). A second centrifugation step was performed to ensure maximal removal of the supernatant, and the remaining RNA pellets were left to air- dry for 3 minutes. Dried RNA pellets were re-suspended in 50 µl of DEPC H_2O and incubated at 65°C for 5 minutes.

To remove any possible DNA contaminants, each sample was incubated (30 minutes, 37°C) with 5 µl DNase buffer and 1 µl of 2 U/ml DNAse I (Life Technologies Inc., Burlington, ON, Canada). To inactivate DNAse activity, 5 µl of DNAse I inactivation

reagent (Life Technologies Inc., Burlington, ON, Canada) was added and samples were mixed by inversion for 2 minutes. Finally, samples were centrifuged (10 000 x g, 10 minutes, 4°C) and the solubilized-RNA supernatants were stored in -80°C until further use.

RNA quantification

RNA samples were thawed on ice, and quantified using the Quant-it Ribogreen RNA assay kit (Life Technologies Inc., Burlington, ON, Canada). 16S/23S rRNA diluted with Tris-EDTA (TE) buffer (10 mM Tris pH 8, 1 mM EDTA) was used as a standard. Samples were diluted 100-fold with TE buffer. Samples were prepared in triplicate, using 1 µl of diluted sample adjusted to a final volume of 100 µl using TE buffer. Samples and standards were prepared directly in a black 96 well microplate. Next, 100 µl of ribogreen solution was added to each well, incubated 2.5 minutes, and fluorescence was measured (485 nm excitation, 520 nm emission) using a FLUOstar Galaxy plate reader.

Reverse transcription and quantitative PCR

To denature RNA samples, a mixture containing 0.5-2 µg of RNA, 5 µl of 0.5 µg/µl random primers (adjusted to a final volume of 30 µl with nuclease-free double-distilled H_2O) was heated at 85°C for 3 minutes then cooled on ice. Using 1x reverse transcription (RT) buffer (50 mM Tris, 75 mM KCl, 3 mM $MgCl_2$ and 5 mM DTT), a RT mastermix (RT+; 1.25 mM dNTPs, 1.4 U/µl RNase OUT, 12.5 U/µl MMLV-RT, in RT buffer) and a negative control (RT-; master mix without MMLV-RT) were prepared. To generate cDNA, 12 µl of denatured RNA/random primer samples were mixed with 8 µl of RT+ and RT- mixes,

respectively. RT+ and RT- mixes were incubated at 42°C for 60 minutes and the reaction was stopped by heating at 92°C for 10 minutes. The cDNA samples were stored in -20°C until use for qPCR.

Thin wall glass capillary tubes (Roche, Laval, QC, Canada) were loaded with 2 µl of cDNA (RT+ or RT-), 10 µl of 2x SYBR Green Reagent (Qiagen, Venlo, LI, Netherlands). 2 µl of 9 µM primers and 6 µl of nuclease-free double-distilled (dd) H_2O. Endogenous controls were prepared with 1 µl Taqman 18S primers, 10 µl 2x Probe Reagent (Qiagen, Venlo, LI, Netherlands), 7 µl of nuclease-free ddH_2O and 2 µl of the 1000x fold diluted cDNA sample. The primers used were as follows: human TNF-α forward primer: GCCCCCAGAGGGAAGAGTTCCC, reverse primer: CAGCTCCACGCCATTGGCCA; human MCP-1 forward primer: CAGCCAGATGCAATCAATGC, GTGGTCCATGGAATCCTGAA, reverse primer; human IL-1β forward primer: GATGAAGTGCTCCTTCCAGGACCT, TGCTGTGAGTCCCGGAGCGT, reverse primer; human IL-6 forward primer: TCCACAAGCGCCTTCGGTCC, TGTCTGTGTGGGGCGGCTACA, reverse primer. Capillaries were centrifuged (700 x g; 1 minute) and placed into a Roche Light Cycler (Roche, Laval, QC, Canada). The PCR reaction conditions were as follows: 95°C for 15 minutes, 45 cycles of 95°C for 15 seconds, 60°C for 30 seconds and 72°C for 30 seconds. Melting curve parameters were as follows: 1 cycle of 95°C for 60 seconds (slope 20°C/sec), 60°C for 60 seconds (slope 20°C/sec), 95°C (slope 0.05°C/sec) and 40°C for 60 seconds (slope 20°C/sec).

Triglyceride extraction and quantification

Day 14 adipocytes were rinsed with ice cold PBS and intracellular TG was solubilized by incubating cells in 1 ml isopropanol-heptane (mixture of 2:3, v/v) for 30 minutes at room temperature. To ensure maximal TG extraction, this process was repeated a second time (500 µl for 15 minutes), transferring solubilized TG to their respective glass tubes after each extractions. The TG extracts were dried using a speed vacuum or with an N_2 stream and stored at -20°C until further use. Prior to quantification, TG extracts were re-suspended in equal volumes of isopropanol. Briefly, samples were prepared in triplicate using either 10 µl of differentiated samples (adjusted with isopropanol to a final volume of 60 µl) or 60 µl of undifferentiated controls, and Triolein was used as a standard. Each sample was dried for 120 minutes in a speed vacuum, then incubated in 250 µl of Infinity Reagent (Thermo Scientific) on a Nutator mixer (90 minutes, 37°C). Finally, samples were transferred to a 96-well microplate and absorbance was read at 540 nm with a FLUOstar Galaxy plate reader. Measured TG levels were normalized to total protein content.

Statistical analysis

Data are represented means ± standard error. Statistical significance was evaluated by a two-way analysis of variance (ANOVA) and differences between means were assessed with Tukey's post hoc test. $P < 0.05$ was considered significant.

RESULTS

Chronic insulin and/or high glucose on insulin signaling

To investigate the effects of chronic insulin and/or high glucose on human primary preadipocytes, confluent preadipocytes were pre-incubated in nutrient stress conditions for 48 hours (5 mM or 25 mM glucose ± 0.6 nM insulin) and then acutely stimulated with 100 nM insulin (or 0.01 N HCl vehicle) for different times periods, as indicated. The acutely stimulated and basal (vehicle treated) responses of cells pre-incubated in 5 mM glucose (normal response) were compared to cells in 5 mM glucose + 0.6 nM insulin and 25 mM glucose ± 0.6 nM insulin conditions.

Chronic insulin and/or high glucose on IR-β tyrosine phosphorylation

I first investigated whether nutrient stress impaired signaling at the level of IR-β. Levels of IR-β Tyr phosphorylation were determined by immunoprecipitation of total cell lysates with anti-phospho-Tyr antibody and then immunoblotting for IR-β (**Fig. 1A**).

In the normal response condition (5 mM glucose pre-incubation), basal levels of Tyr phosphorylated IR-β were minimal and increased significantly, following acute insulin stimulation (**Fig. 1A**). Similarly, acute stimulation in both the 5 mM glucose + 0.6 nM insulin and the 25 mM glucose conditions, yielded significantly increased levels of IR-β Tyr phosphorylation, when compared to their respective basal values. There was no significant insulin-stimulated increase of IR-β Tyr phosphorylation with the 25 mM glucose + 0.6 nM insulin condition. Comparing the stimulated responses relative to the normal 5 mM glucose

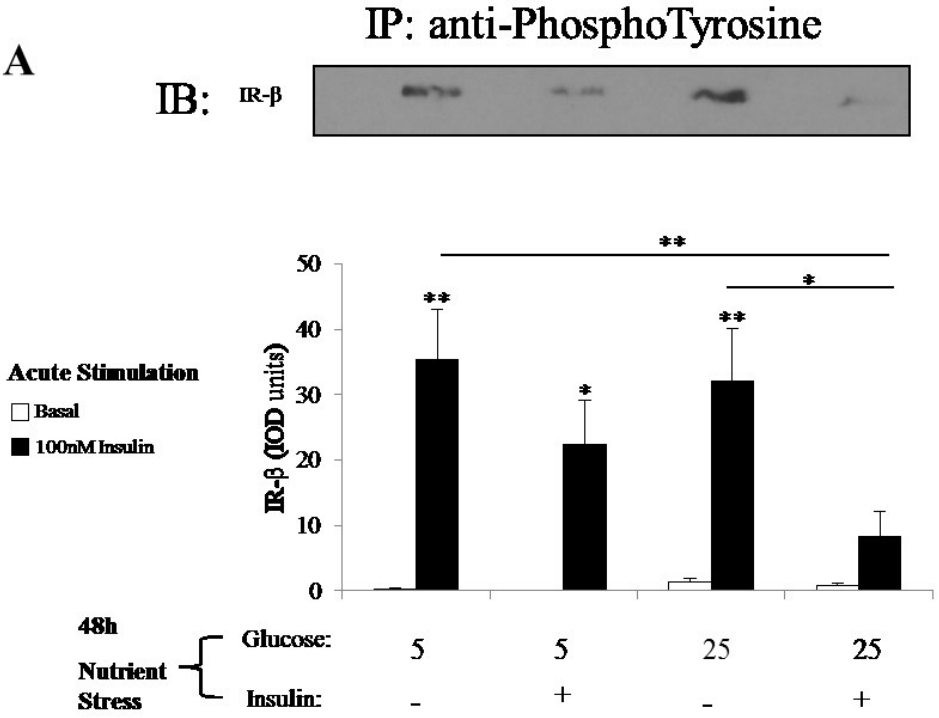
A
IP: anti-PhosphoTyrosine
IB:
IR-β
**
*
**
*
**
50
40
30
20
10
0
IR-β (IOD units)
Acute Stimulation
Basal
100nM Insulin
48h
Nutrient Stress
Glucose:
5
5
25
25
Insulin:
-
+
-
+

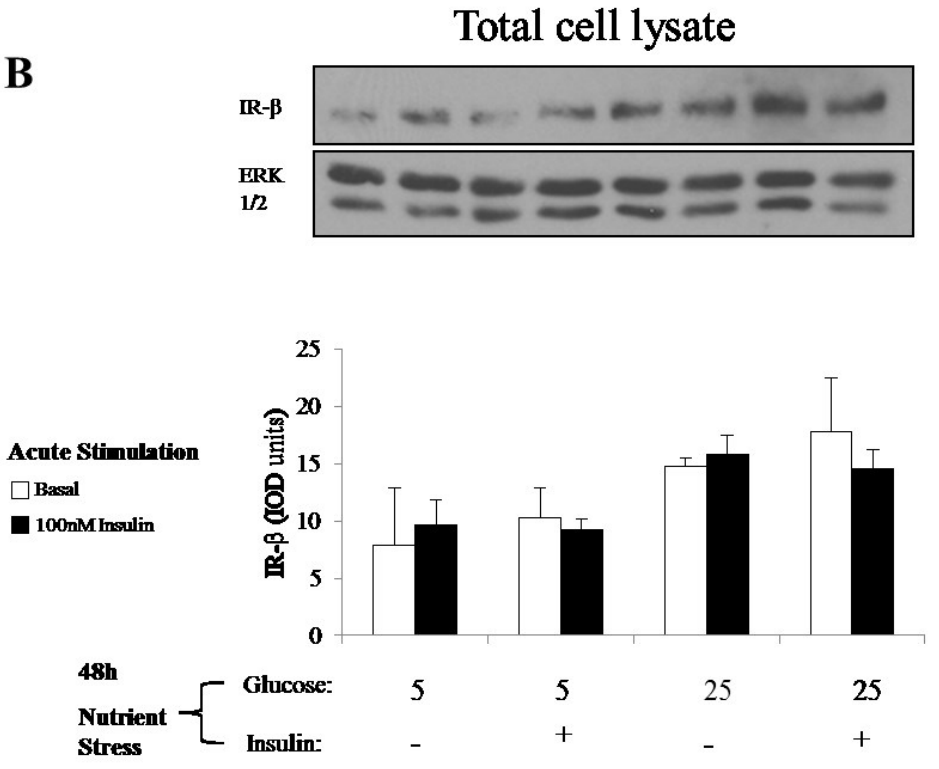
B
Total cell lysate
IR-β
ERK 1/2
25
20
15
10
5
0
IR-β (IOD units)
Acute Stimulation
Basal
100nM Insulin
48h
Nutrient Stress
Glucose:
5
5
25
25
Insulin:
-
+
-
+

Figure 1. ***25 mM glucose and 0.6 nM insulin for 48 hours decreases insulin-stimulated IR-β tyrosine phosphorylation in human preadipocytes.*** Following pre-treatment, preadipocytes were stimulated with 100 nM insulin (or HCl vehicle) for 5 minutes. Cells were lysed and in (A), extracted protein was immunoprecipitated using anti-phosphotyrosine antibody. Immunoprecipitated proteins (A) and proteins from total cell lysates (B) were separated by SDS-PAGE and immunoblotted with anti- IR-β antibody. Data in (A) and (B) represent mean ± SE from 5 and 3 independent experiments, respectively. Representative blots are shown in top panels for (A) and (B). Statistical analysis was by two-way ANOVA with Tukey's post-hoc tests. ** $p < 0.01$, *$p < 0.05$, versus basal or between indicated pairs. There were no statistical differences between treatment conditions in (B).

response, neither the 25 mM glucose nor the 5 mM glucose + 0.6 nM insulin pre-incubation conditions demonstrated an inhibition in Tyr phosphorylation of IR-β (**Fig. 1A**). In contrast, the effect of 25 mM glucose + 0.6 nM insulin pre-incubation resulted in a significant 76.7 % reduction, relative to the normal response (**Fig. 1A**). This inhibition was neither BMI nor age dependent. The reduction in the signaling response was not due to protein degradation, as shown by stable levels of IR-β expression in total cell lysates (**Fig. 1B**).

Chronic insulin and/or high glucose on IRS-1 tyrosine phosphorylation

We next investigated whether the nutrient stress-mediated impairment of IR-β Tyr phosphorylation would also impair IRS-1 Tyr phosphorylation.

As expected, in the normal response basal levels of Tyr phosphorylated IRS-1 were minimal and increased significantly following acute insulin stimulation. There were no significant increases in IRS-1 Tyr phosphorylation with acute stimulation in the 25 mM glucose ± 0.6 nM insulin conditions, relative to their respective basal values (**Fig. 2A**).

Comparing levels of acutely stimulated responses relative to the normal 5 mM glucose response (**Fig. 2A**), 5 mM glucose + 0.6 nM insulin, 25 mM glucose, and the combination condition, all displayed significant reductions of IRS-1 Tyr phosphorylation (reductions of 66.3 %, 65.9 % and 81.4 %, respectively). Consistent with the IR-β findings, inhibition was neither BMI nor age dependent. Similarly, the reductions were not due to protein degradation, as shown by stable levels of IRS-1 expression in total cell lysates (**Fig. 2B**).

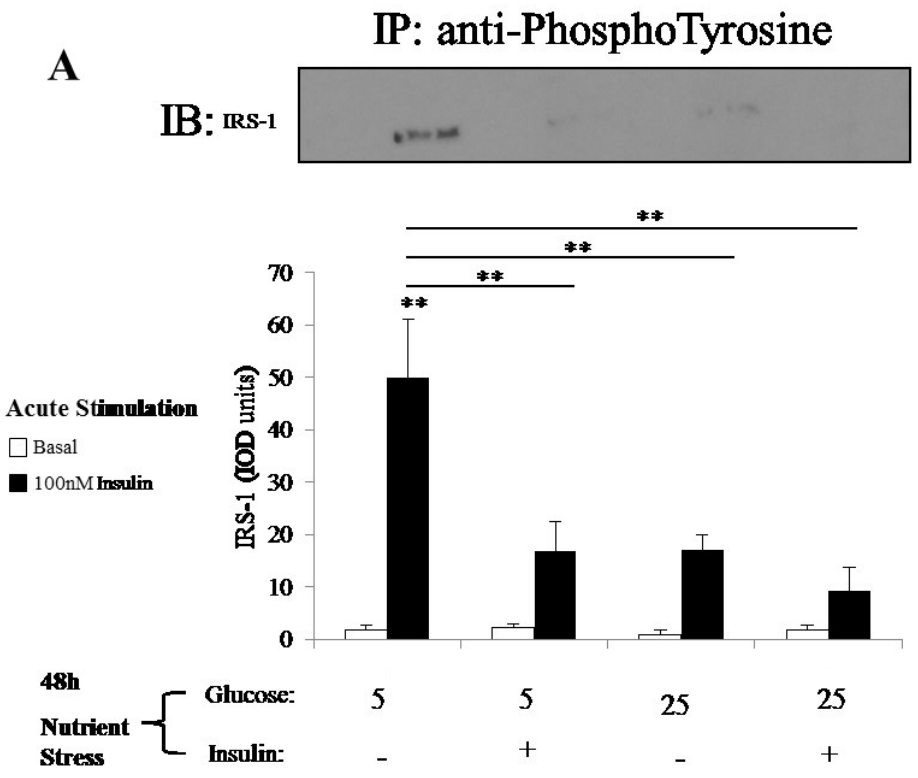
A
IP: anti-PhosphoTyrosine
IB: IRS-1
**
**
**
**
70
60
50
40
30
20
10
0
IRS-1 (IOD units)
Acute Stimulation
Basal
100nM Insulin
48h
Nutrient Stress
Glucose:
5
5
25
25
Insulin:
-
+
-
+

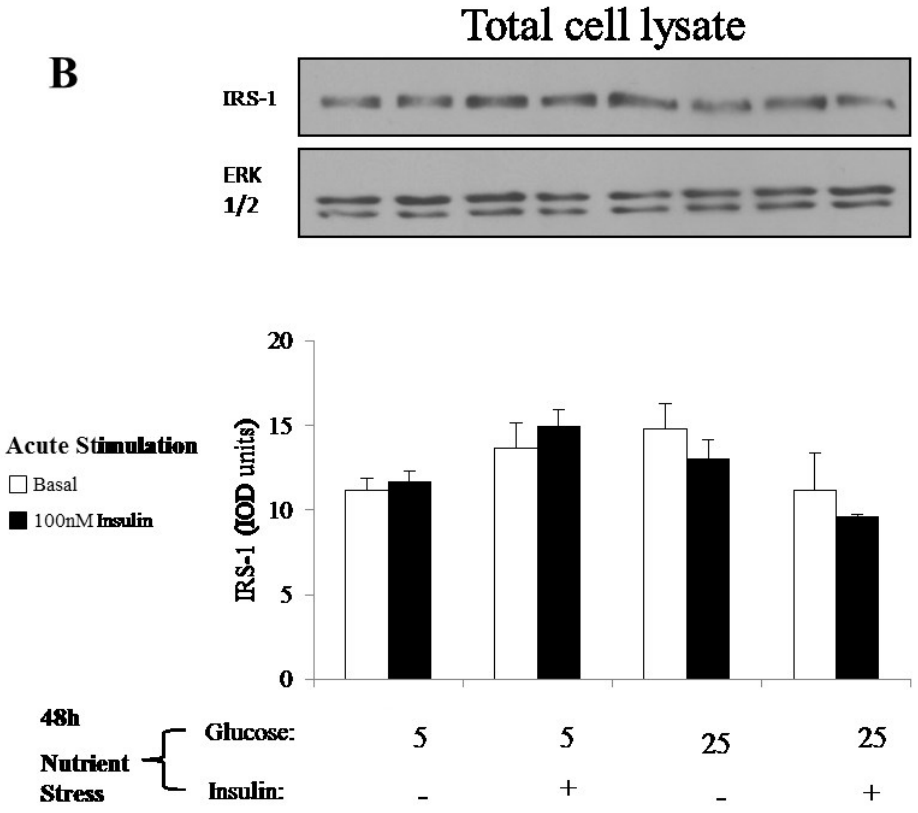
B
Total cell lysate
IRS-1
ERK 1/2
20
15
10
5
0
IRS-1 (IOD units)
Acute Stimulation
Basal
100nM Insulin
48h
Nutrient Stress
Glucose:
5
5
25
25
Insulin:
-
+
-
+

Figure 2. ***25 mM glucose and 0.6 nM insulin for 48 hours decreases insulin-stimulated IRS-1 tyrosine phosphorylation in human preadipocytes***. Following pre-treatment, preadipocytes were stimulated with 100 nM insulin (or HCl vehicle) for 5 minutes. Cells were lysed and in (A), extracted protein was immunoprecipitated using anti-phosphotyrosine antibody. Immunoprecipitated proteins (A) and proteins from total cell lysates (B) were separated by SDS-PAGE and immunoblotted with anti- IRS-1 antibody. Data in (A) and (B) represent mean ± SE from 4 and 3 independent experiments, respectively. Representative blots are shown in top panels for (A) and (B). Statistical analysis was by two-way ANOVA with Tukey's post-hoc tests. ** $p < 0.01$, versus basal or between indicated pairs. There were no statistical differences between treatment conditions in (B).

Chronic insulin and/or high glucose on Ser^{473} Akt phosphorylation

To investigate whether the insulin and high glucose stress-mediated impairment of IR-β and IRS-1 extended to phosphorylation of Akt, preadipocytes were acutely stimulated with 100 nM insulin for 5 minutes following the 48 hour nutrient stress, proteins were solubilized and lysates were immunoblotted for Akt and Ser^{473} phosphorylated Akt (pAkt).

In all treatment conditions, following acute insulin stimulation, levels of Ser^{473} pAkt normalized to Akt (Ser^{473} pAkt /Akt) increased significantly relative to their respective basal values (**Fig. 3**). Comparing the acutely-stimulated responses, Ser^{473} pAkt /Akt levels were not significantly different across the 4 different conditions.

With 15 minute acute stimulation, levels of Ser^{473} pAkt/Akt in the 5 mM glucose and 25 mM glucose conditions were significantly increased relative to their respective basal values (**Fig 4**). Furthermore, these levels were not significantly increased after stimulation in either of the 0.6 nM insulin conditions. No significant differences between the acutely stimulated responses were found.

Chronic insulin and/or high glucose on pro-inflammatory cytokine expression

To investigate the effect of high glucose and chronic insulin on pro-inflammatory adipokine expression in preadipocytes, RNA was extracted immediately following the 48 hour pre-incubation conditions described above. Next, IL-6, MCP-1, TNF-α, and IL-1β mRNA expression levels were quantified via real-time-qPCR (**Fig. 5**). Levels of these pro-inflammatory adipokines were not significantly different across the 4 different conditions.

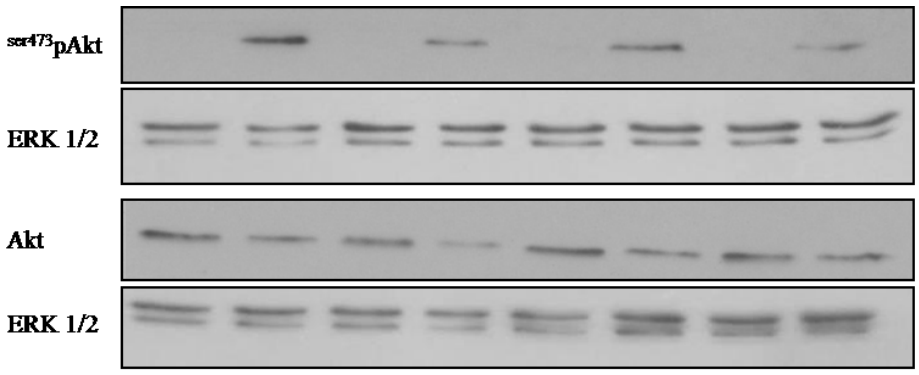
ser473pAkt
ERK 1/2
Akt
ERK 1/2

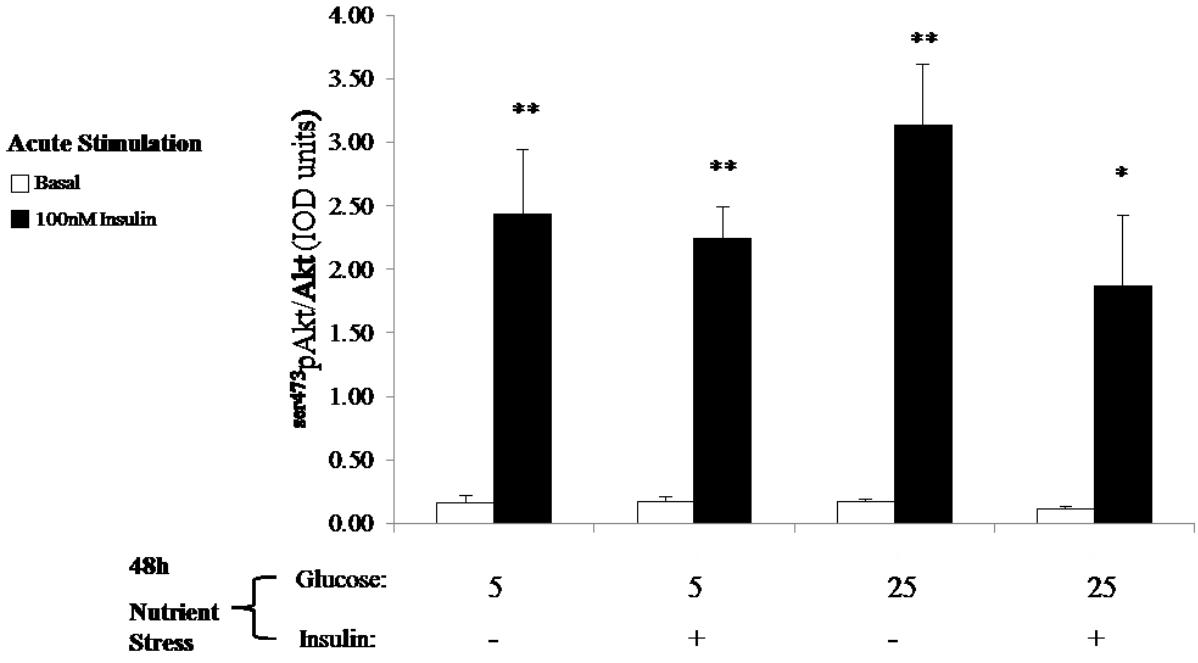
Acute Stimulation
Basal
100nM Insulin
ser473pAkt/Akt (IOD units)
4.00
3.50
3.00
2.50
2.00
1.50
1.00
0.50
0.00
**
**
**
*
48h
Nutrient Stress
Glucose:
5
5
25
25
Insulin:
-
+
-
+

Figure 3. ***25 mM glucose and 0.6 nM insulin for 48 hours does not change levels of insulin-stimulated serine-473 Akt phosphorylation at 5 minutes in human preadipocytes.*** Following pre-treatment preadipocytes were stimulated with 100 nM insulin (or HCl vehicle) for 5 minutes. After cell lysis, extracted protein was separated by SDS-PAGE and immunoblotted with anti-Akt or anti- phospho-serine 473 Akt (pAkt) antibody. Representative blots are shown in top panel, with ERK 1/2 shown as a loading control. Data represent pAkt (normalized to Akt) from 5 independent experiments (mean ± SE). Statistical analysis was by two-way ANOVA with Tukey's post-hoc tests. ** $p < 0.01$, *$p < 0.05$, versus basal or between indicated pairs.

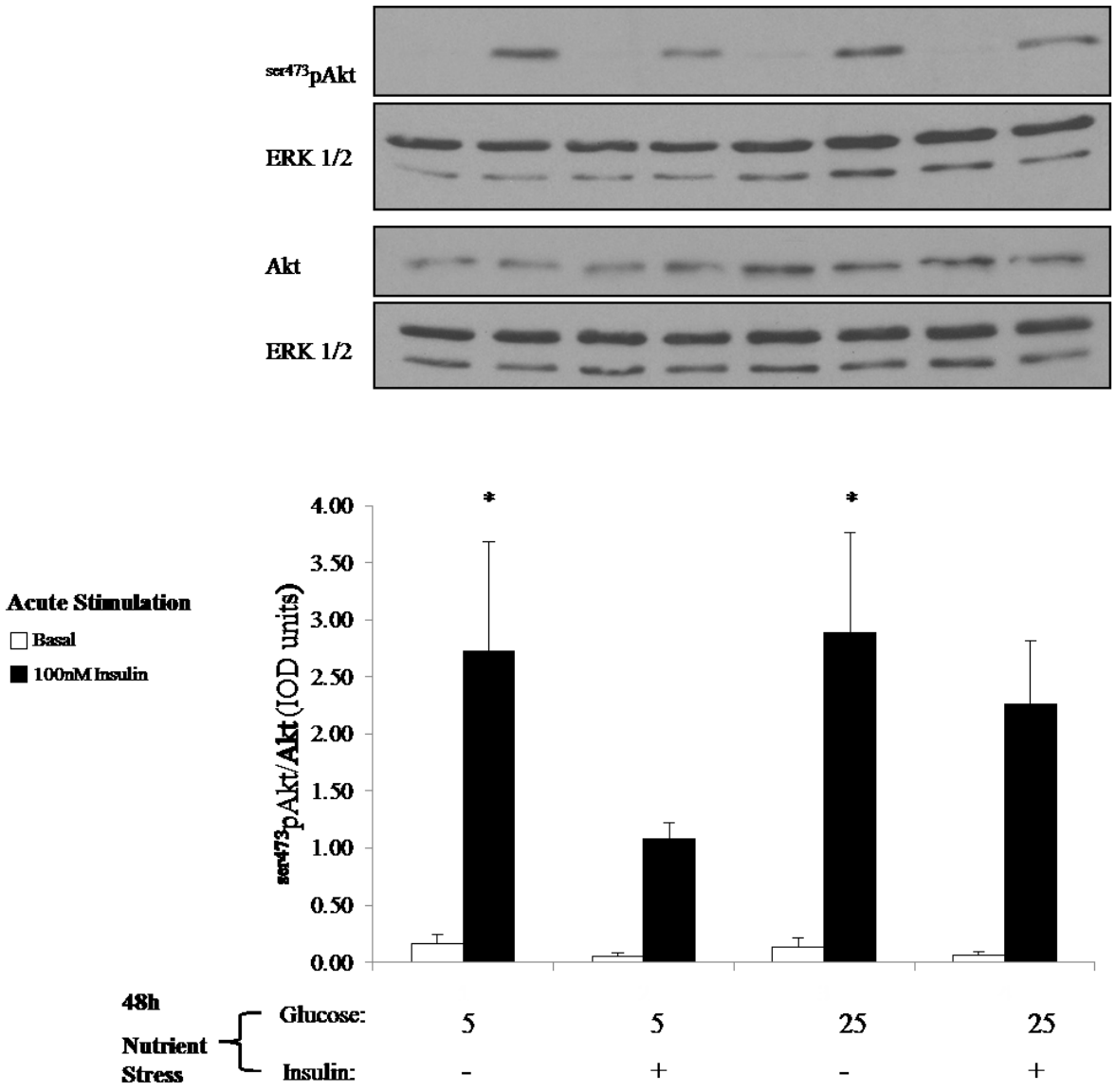
ser473pAkt
ERK 1/2
Akt
ERK 1/2
Acute Stimulation
Basal
100nM Insulin
ser473pAkt/Akt (IOD units)
4.00
3.50
3.00
2.50
2.00
1.50
1.00
0.50
0.00
*
*
48h
Nutrient Stress
Glucose:
5
5
25
25
Insulin:
-
+
-
+

Figure 4. ***25 mM glucose and 0.6 nM insulin for 48 hours does not change levels of insulin-stimulated serine-473 Akt phosphorylation at 15 minutes in human preadipocytes.*** Following pre-treatment preadipocytes were stimulated with 100 nM insulin (or HCl vehicle) for 15 minutes. After cell lysis, extracted protein was separated by SDS-PAGE and immunoblotted with anti-Akt or anti- phospho-serine 473 Akt (pAkt) antibody. Representative blots are shown in top panel, with ERK 1/2 shown as a loading control. Data represent pAkt (normalized to Akt) from 3 independent experiments (mean ± SE). Statistical analysis was by two-way ANOVA with Tukey's post-hoc tests. *$p < 0.05$. (*) indicates significance versus basal.

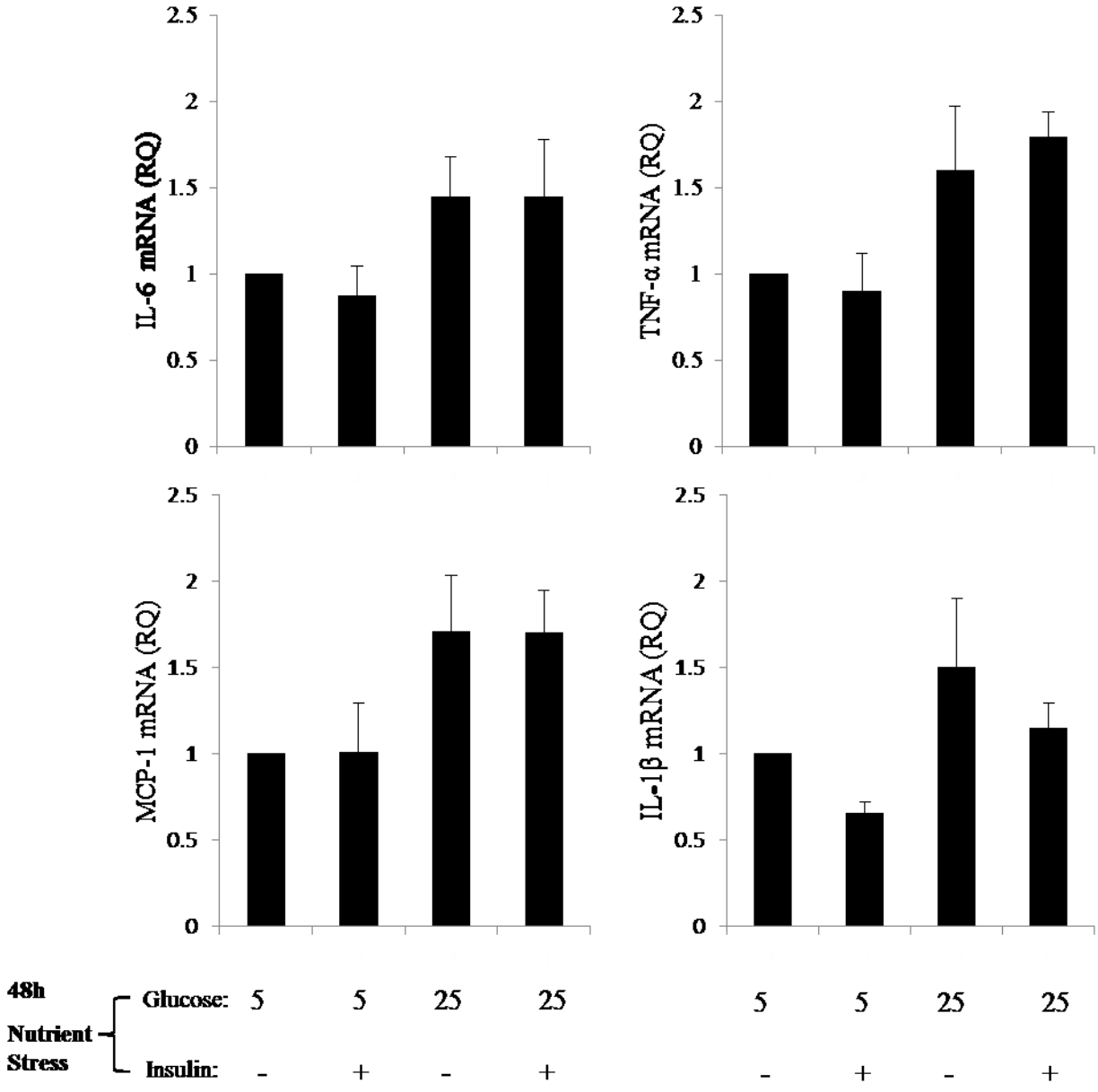
IL-6 mRNA (RQ)
TNF-α mRNA (RQ)
MCP-1 mRNA (RQ)
IL-1β mRNA (RQ)
2.5
2
1.5
1
0.5
0
48h
Nutrient Stress
Glucose: 5 5 25 25
Insulin: - + - +

Figure 5. ***25 mM glucose and 0.6 nM insulin for 48 hours does not change levels of pro-inflammatory markers in human preadipocytes*****.** Following 48 hour nutrient stress, RNA was extracted using Qiazol reagent. The mRNA expression was determined using qPCR with 18S as an endogenous control. IL-6 and MCP-1 represent data from 4 independent experiments, TNF-α and IL-1β represent data from 3 independent experiments (mean ± SE). Statistical analysis was by two-way ANOVA with Tukey's post-hoc tests. There were no statistical differences between treatment conditions.

Effect of chronic insulin and/or high glucose on adipogenesis

Following the 48 hour nutrient stress treatment, cells were differentiated in media containing either 5 mM or 25 mM glucose (**Fig. 6 and Fig. 7**). On day 14 of differentiation, triglycerides (TG) were extracted, and cellular protein was collected. Solubilized protein was immunoblotted for adipogenic markers: PPARγ, SREBP-1 and FAS.

Despite the inhibition of acute insulin signaling at the level of IR-β and IRS-1, there was no effect on intracellular TG accumulation (**Fig. 6B**). Minimal TG accumulation was observed in the undifferentiated controls. Finally, levels of the adipogenic markers (PPARγ, SREBP-1 and FAS) also did not vary significantly between the various treatment conditions (**Fig. 7**).

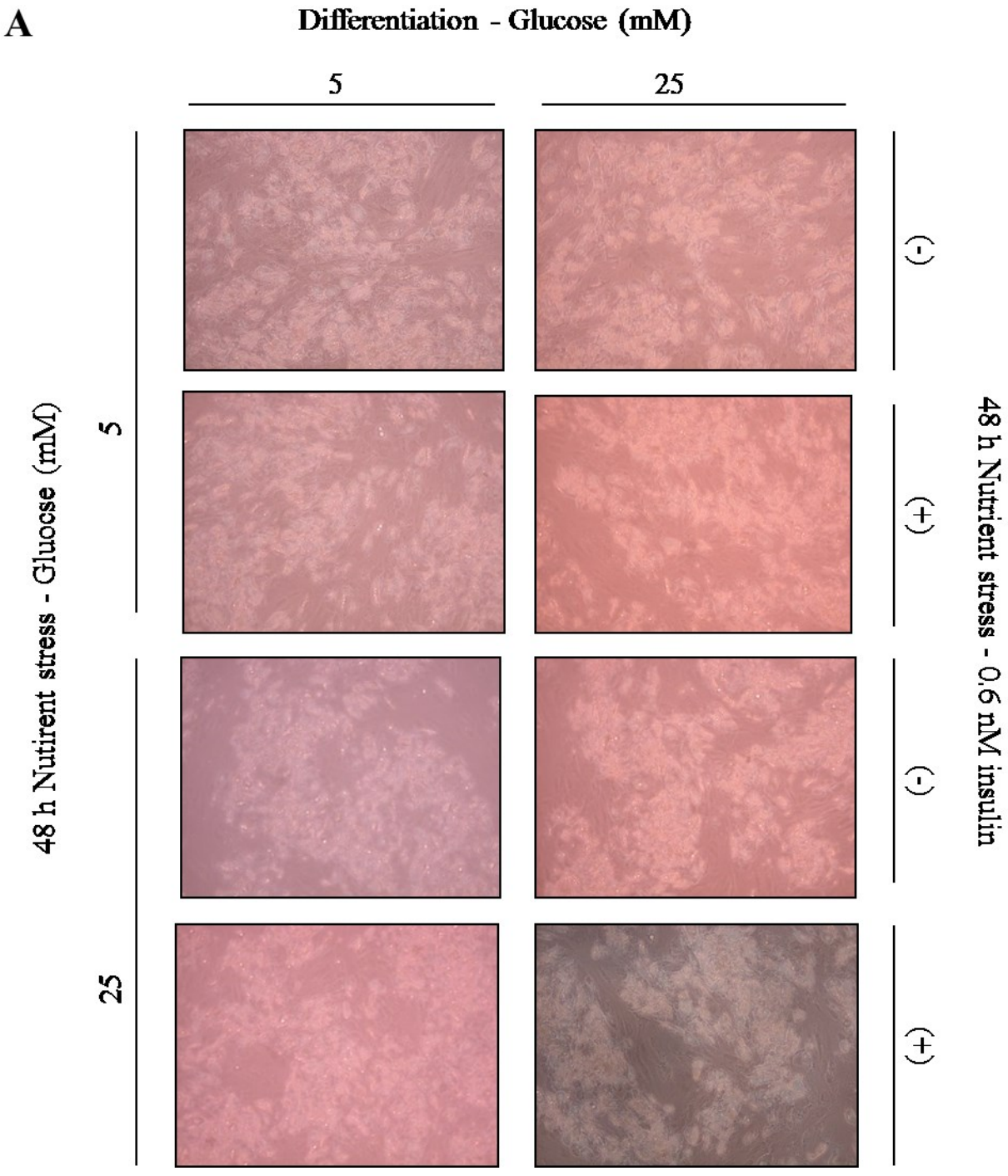
A
Differentiation - Glucose (mM)
5
25
48 h Nutirent stress - Gluocse (mM)
5
25
48 h Nutrient stress - 0.6 nM insulin
(-)
(+)
(-)
(+)

B

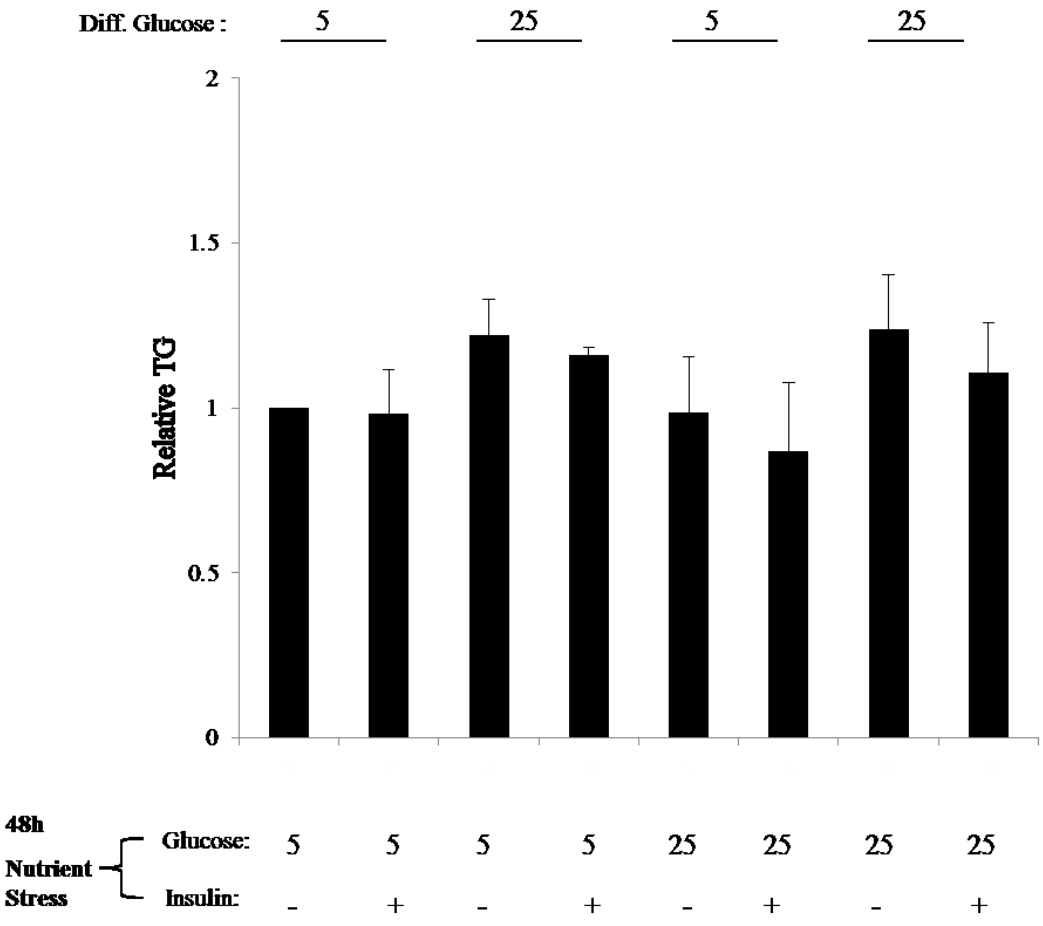
Diff. Glucose :
5
25
5
25
2
1.5
1
0.5
0
Relative TG
48h
Nutrient Stress
Glucose:
5 5 5 5 25 25 25 25
Insulin:
- + - + - + - +

Figure 6. ***25 mM glucose and 0.6 nM insulin for 48 hours prior to differentiation does not change accumulation of triglyceride in human adipocytes.*** Preadipocytes were pre-treated for 48 hours (5 mM/25 mM glucose ± 0.6 nM insulin) prior to a 14 day of differentiation in adipogenic cocktail containing 5 mM/ 25 mM glucose. Prior to triglyceride (TG) extraction on day 14, photomicrographs of each treatment condition were taken and are as shown in (A). TG were extracted from differentiated adipocytes and quantified in (B). Data in (B) represent TG (μg)/protein (mg) normalized to lane 1 (mean ± SE, from 3 independent experiments). Statistical analysis was by two-way ANOVA with Tukey's post-hoc tests. There were no statistical differences between treatment conditions.

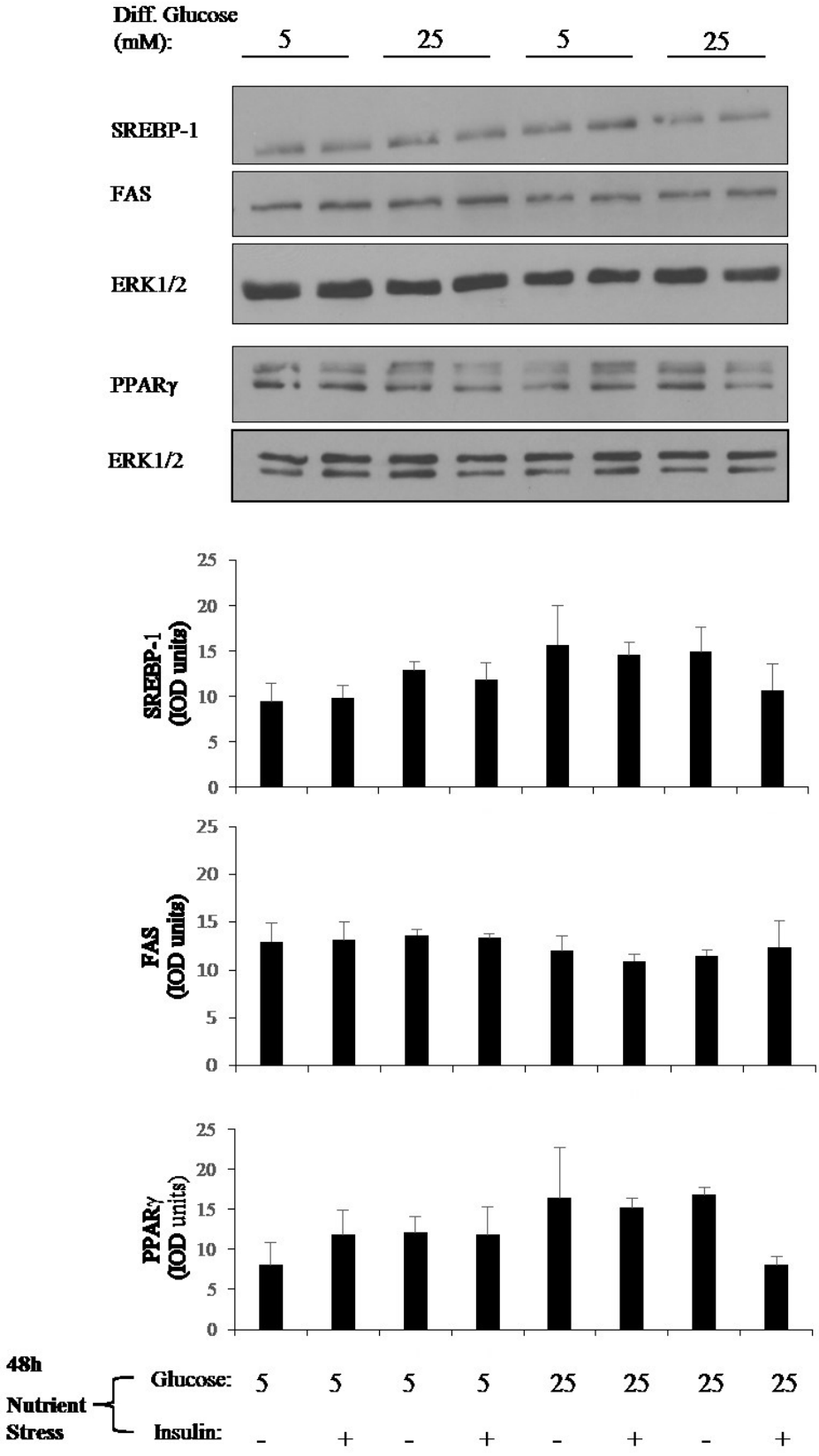
Diff. Glucose (mM):
5
25
5
25
SREBP-1
FAS
ERK1/2
PPARγ
ERK1/2
SREBP-1 (IOD units)
FAS (IOD units)
PPARγ (IOD units)
0
5
10
15
20
25
48h
Nutrient Stress
Glucose:
5 5 5 5 25 25 25 25
Insulin:
- + - + - + - +

Figure 7. ***25 mM glucose and 0.6 nM insulin for 48 hours prior to differentiation does not change levels of adipogenic markers in human adipocytes*****.** Preadipocytes were pre-treated for 48 hours (5 mM/25 mM glucose ± 0.6 nM insulin) prior to a 14 day of differentiation in adipogenic cocktail containing 5 mM/ 25 mM glucose. At day 14, proteins were extracted from adipocytes, separated by SDS-PAGE and immunoblotted with anti- SREBP1, anti-Fatty Acid Synthase (FAS) and anti-Peroxisome Proliferator-Activated Receptor (PPAR)-γ antibody. Representative blots are in the top panel, with ERK 1/2 shown as a loading control. Data represent mean± SE from 3 independent experiments. Statistical analysis was by two-way ANOVA with Tukey's post-hoc tests. There were no statistical differences between treatment conditions.

DISCUSSION

Studies using insulin and high glucose-based nutrient stress focus mainly on the adipocyte. Given the importance of insulin signaling in the adipocyte, findings from these mature cell studies still provide important points of comparison with the present study on preadipocytes.

The preadipocyte is critical for healthy AT remodeling and function. However, there are few studies that describe the effects of high glucose-based nutrient stress on these cells, and even fewer using human preadipocytes. We therefore investigated whether chronic exposure to high glucose and/or 0.6 nM insulin would impair insulin signaling and differentiation of human preadipocytes.

Chronic insulin and high glucose on insulin signaling

The effects of chronic insulin and/or high glucose on IR-β and IRS-1

My data demonstrate decreased insulin-stimulated IR-β Tyr phosphorylation in human preadipocytes chronically exposed to high glucose + 0.6 nM insulin. Consistent with this, adipocytes from patients with T2D exhibit reduced IR Tyr kinase activity (Freidenberg et al., 1987). Furthermore, chronic exposure of isolated rat adipocytes to high insulin (100 nM) and hyperglycemia results in attenuation of insulin-stimulated IR-β Tyr phosphorylation (Tang et al., 2001). However, in contrast with my findings, other studies with 3T3-L1 adipocytes and isolated rat adipocytes cultured in low dose insulin (5 nM and 8.6 nM, respectively) and high glucose report no effect on insulin-stimulated IR-β Tyr

phosphorylation (Lima et al., 1991; Ross et al., 2000). Variations in insulin concentration may play a role in the attenuation of the IR-β response in the adipocyte, and these findings may diverge from my own owing to the fact that they used 3T3-L1 and rat adipocytes, versus the human preadipocytes I used.

Rat-1 fibroblasts (established from F2408 rat embryos) are highly transfectable 3T3-like cells, and were first described in 1976 (Prasad et al., 1976; Topp, 1981). Since then, several studies have examined the insulin-stimulated responses of Rat-1 fibroblasts overexpressing the human insulin receptor (Rat-1 HIRcBs) following exposure to high glucose. Exposure of Rat-1 HIRcBs to high glucose impairs IR-β insulin-stimulated Tyr phosphorylation (Berti et al., 1994; Maegawa et al., 1995; Pillay et al., 1996). I found that high glucose alone had no effect on this response. However, I observed synergistic inhibition with high glucose + 0.6 nM insulin. Individually, neither component alone significantly reduced insulin-stimulated Tyr phosphorylation of IR-β. Differences between human preadipocytes versus rat fibroblasts expressing high levels of human insulin receptor may account for this variation.

Phosphorylation of Tyr^{960} within the NPXY motif of IR-β enables binding of the IRS-1 N-terminal PTB domain, thus permitting the insulin signaling cascade to continue (Ramalingam et al., 2013; White et al., 1988). Therefore, I investigated whether the attenuation at the level of IR-β would affect insulin-stimulated Tyr phosphorylation of IRS-1. Levels of insulin-stimulated IRS-1 Tyr phosphorylation were decreased with 25 mM glucose and/or 0.6 nM insulin. Consistent with my findings, 3T3-L1 preadipocytes incubated overnight in 25 mM glucose display reduced insulin-stimulated IRS-1 Tyr phosphorylation (Gagnon and Sorisky, 1998). Similarly, Rat-1 HIRcBs exposed to high glucose exhibit

reduced insulin-stimulated IRS-1 Tyr phosphorylation (Berti et al., 1994; Maegawa et al., 1995; Pillay et al., 1996). In contrast to these studies, mature 3T3-L1 adipocytes and isolated rat adipocytes exposed to low dose insulin and high glucose do not exhibit attenuated insulin-stimulated IRS-1 Tyr phosphorylation (Lima et al., 1991; Ross et al., 2000). Differences in the data may be due to divergent responses between the mature and undifferentiated cells.

My data demonstrate that the insulin-stimulated IRS-1 Tyr phosphorylation response is more sensitive to the high glucose and/or 0.6 nM insulin nutrient stress than is IR-β, as either high glucose or 0.6 nM insulin alone could attenuate the response. The insulin-stimulated high glucose + 0.6 nM insulin condition demonstrated similar decreases in Tyr phosphorylation as with each component individually, suggesting an absence of synergy that was previously described with IR-β. The lack of synergistic effect at the level of IRS-1 Tyr phosphorylation might be because each condition alone was quite potent in causing inhibition of the response. Similar to my findings, Pillay et al reported that Rat-1 HIRcBs exposed to high glucose alone display greater inhibition of insulin-stimulated Tyr phosphorylation of IRS-1 when compared to IR-β (Pillay et al., 1996). The mechanism for this effect might involve increased Ser kinase activity directed against IRS-1 and/or increased Tyr dephosphorylation of IRS-1 by PTPs, compared to IR.

Ser phosphorylation of IRS-1 can induce conformational changes that disrupt insulin signaling by preventing the interactions between the IRS-1 PTB and IR-β, and therefore lead to reduced IRS-1 tyrosine phosphorylation (Paz et al., 1997). PKC can phosphorylate IRS-1 at Ser residues, and high glucose has been reported to induce its activity (Draznin, 2006; Idris et al., 2001). Disruption of IR-β/IRS-1 PTB interactions via Ser phosphorylation of IRS-1, might explain the reduction in insulin-stimulated IRS-1 Tyr phosphorylation despite the

absence of inhibition at the level of IR-β in the individual high glucose/0.6 nM insulin conditions. To this end, measuring the Ser phosphorylation status of IRS-1 in future experiments may elucidate specific mechanisms by which this protein is differentially inhibited when compared to IR-β.

Several studies report increased PTP activity in Rat-1 fibroblasts and 3T3-L1 preadipocytes exposed to high glucose (Gagnon and Sorisky, 1998; Shimizu et al., 2002). In 3T3-L1 preadipocytes, high glucose-induced attenuation of IRS-1 Tyr phosphorylation coincides with increased expression of leukocyte antigen-related (LAR) PTP (Gagnon and Sorisky, 1998). IRS-1 may be preferentially targeted by PTPs in the individual high glucose/0.6 nM insulin conditions in the present study. More work will be needed to determine if this is the case.

My data demonstrate that the reductions of IR-β and IRS-1 Tyr phosphorylation were not due to protein degradation, as shown by stable protein levels in total cell lysates. The proteasomal degradation of IRS-1 has been previously described in 3T3-L1 adipocytes treated with high glucose and high insulin (20 nM), however, this does not occur with 0.6 nM insulin (Robinson and Buse, 2008).

The effects of chronic insulin and/or high glucose on Akt

Little is known regarding the effects of high glucose based stress on Akt in the human preadipocyte. Using isolated human SC preadipocytes, Moreno-Navarrete found a significant inhibition of insulin-stimulated Ser^{473} Akt phosphorylation in cells pre-incubated 48 hours with 100 mM glucose, however, this concentration of glucose is unusually high (Moreno-Navarrete et al., 2013). Alternatively, in mature 3T3-L1 adipocytes, inhibition of insulin-

stimulated Ser^{473} Akt phosphorylation occurs following a 24 hour exposure to high glucose and 0.6 nM insulin (Robinson et al., 2014). I observed no significant changes in Ser^{473} Akt phosphorylation following 48 hour exposure of human preadipocytes to high glucose and/or 0.6 nM insulin, with 5 minutes of acute insulin stimulation. It should be noted that a ~22% inhibition of Akt phosphorylation was observed in the high glucose + 0.6 nM insulin condition at the 5 minute stimulation time point, however, possibly due to variations between patient responses, this inhibition was not statistically significant.

Previous 3T3-L1 adipocyte studies using the 25 mM glucose and/or 0.6 nM insulin conditions measured Akt phosphorylation following 15 minutes of acute insulin stimulation (Nelson et al., 2000; Robinson and Buse, 2008; Robinson et al., 2014). To explore the possibility that a longer stimulation may be required for the detection of Akt inhibition, and to directly compare findings to 3T3-L1 adipocyte studies, I extended the acute insulin stimulation time to 15 minutes. However, even with the 15 minute acute stimulation, I still observed no inhibition of insulin-stimulated Ser^{473} Akt phosphorylation following chronic exposure to high glucose and/or 0.6 nM insulin.

Akt is activated by two phosphorylation events; an initial phosphorylation at Thr^{308} by PDK1 that partially activates Akt, and a second phosphorylation at Ser^{473} by PI3K/mTORC2 that fully activates it (Tsuchiya et al., 2013). In 3T3-L1 adipocytes, insulin-stimulated Thr^{308} and Ser^{473} Akt phosphorylation are attenuated in parallel with chronic exposure to high glucose and/or 0.6 nM insulin (Nelson et al., 2002). Future studies will be needed to address whether Thr^{308} and Ser^{473} phosphorylation of Akt in human preadipocytes are affected to a similar extent or not.

My findings regarding Akt phosphorylation are unexpected given the inhibition at the level of IR-β/IRS-1 signaling. The absence of inhibition of insulin-stimulated Akt phosphorylation may be due to a sample size limitation. Increasing the sample size may correct for the variations between patient responses and perhaps reveal a BMI and/or age-dependent effect. Alternatively, this lack of inhibition may be due to the time points chosen for acute stimulation, a possibility that could be addressed with time-course studies.

Chronic insulin and/or high glucose on inflammation

Levels of pro-inflammatory adipokines are elevated in the AT of obese patients and those with T2D (Esser et al., 2014). Alternatively, treatment of 3T3-L1 adipocytes with high glucose promotes inflammatory adipokine expression (Koenen et al., 2011; Pan et al., 2014). Pro-inflammatory adipokines interfere with insulin signaling through several mechanisms, including the Ser phosphorylation of IRS-1 and the attenuation of IR-β/IRS-1 Tyr phosphorylation (Shah et al., 2008). To investigate whether the decreases in IR-β or IRS-1 Tyr phosphorylation correlate with inflammation, I measured the expression of pro-inflammatory markers. I found that chronic high glucose and/or 0.6 nM insulin did not increase pro-inflammatory adipokine mRNA expression as assessed by levels of IL-6, MCP-1, TNF-α and, IL-1β. In the high glucose conditions, levels of all four pro-inflammatory markers trended towards an increase, thus, the absence of significant differences may be due to a sample size limitation. It remains to be determined if there are differences in the amount of secreted adipokines.

Chronic insulin and/or high glucose on adipogenesis

Differentiation in high glucose generates hypertrophic and inflamed, insulin-resistant 3T3-L1 adipocytes (Han et al., 2007; Lin et al., 2005). Nevertheless, differentiation and maintenance in cell culture most commonly occurs using 25 mM glucose medium conditions (Tanis et al., 2015). I investigated the extent to which high glucose-based stress prior to and/or during differentiation might influence adipogenesis in the human preadipocyte model. I found no differences in intracellular TG accumulation nor did I find differences in levels of adipogenic markers (i.e. PPARγ, FAS, and SREBP-1) between the treatment conditions. Consistent with my findings, Collins et al report that human SC preadipocytes differentiated in 5 mM versus 17.5 mM glucose do not display significant differences in TG accumulation at day 14 (Collins et al., 2011).

It should be noted that I used hyperinsulinemic conditions to induce adipogenesis (850 nM insulin). Given that our observed attenuation of preadipocyte IR-β/IRS-1 Tyr phosphorylation was measured using 100 nM insulin for 5 minutes, exposure to 850 nM insulin over the 14 days of differentiation may reverse or compensate for any early signaling defects. To this end, future experiments could measure the induction of adipogenic markers at different time points throughout differentiation (especially at early time points), enabling a comparison of the differentiation dynamics between the treatment conditions. The differentiation protocol could be modified to use lower concentrations of insulin to see if that would make the adipogenic process more susceptible to inhibition.

Proposed Model

The IR/IRS-1 axis is crucial for Akt activation and the induction of adipogenesis. Here I report that high glucose + 0.6 nM insulin attenuates acute insulin-stimulated Tyr phosphorylation of both the IR and IRS-1, without having a negative impact on Ser^{473} pAkt levels or pro-inflammatory adipokine expression in the preadipocyte. Similar levels of TG accumulation and adipogenic markers between the different adipogenic treatments is consistent with the absence of inhibition at the level of Akt.

Rat-1 HIRcBs exposed to high glucose exhibit decreased IR-β and IRS-1 Tyr phosphorylation due to increased PTP-1B activity (Maegawa et al., 1995). Overexpression of PTP-1B in Rat-1 HIRcBs results in the attenuation of insulin-stimulated IR-β and IRS-1 Tyr phosphorylation, with only minimal impairment to insulin-stimulated Akt activation (Shimizu et al., 2002). Similarly, overexpression of PTP-1B in 3T3-L1 adipocytes also inhibits insulin-stimulated IR-β and IRS-1 Tyr phosphorylation, with only modest impairment to insulin-stimulated Akt activation (Shimizu et al., 2002; Venable et al., 2000). These studies suggest a mechanism by which chronic exposure of human preadipocytes to high glucose and/or 0.6 nM insulin may activate PTP-1B, and impair insulin-stimulated IR-β and IRS-1 Tyr phosphorylation without affecting Akt activation; this is a hypothesis that could be addressed in future experiments.

Divergent effects between IR-β/IRS-1 and Akt phosphorylation are also seen in primary cultured rat adipocytes exposed to 15 mM glucose + high insulin. They exhibit marked reductions in IRS-1 content, without changes in maximal insulin stimulated Ser^{473} Akt phosphorylation (Buren et al., 2003).

It is possible that, despite marked decreases in insulin-stimulated Tyr phosphorylation I observed, the attenuated IR-β/IRS-1 signals still reach a minimal threshold required for downstream Ser^{473} Akt phosphorylation to persist in human preadipocytes (**Fig. 8**).

Normal Signaling

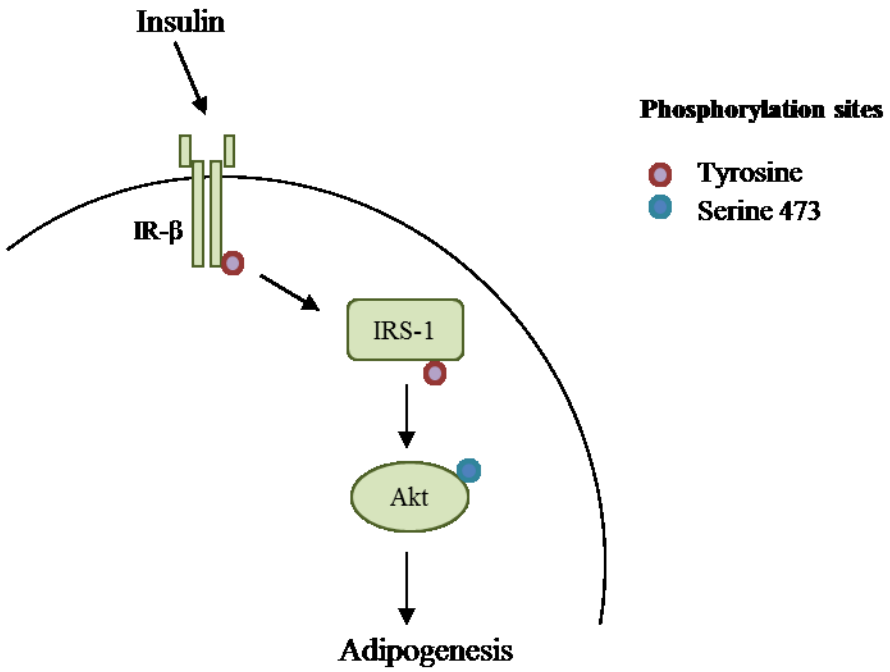

Impaired Signaling

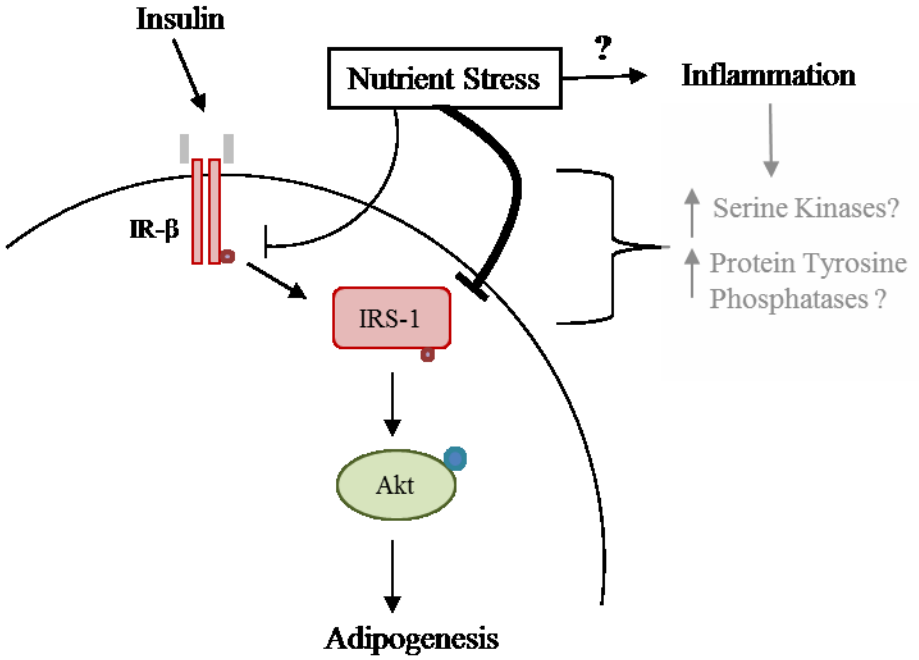

Figure 8. ***Proposed model of attenuation of insulin signaling in the human preadipocyte caused by chronic high glucose and/or 0.6 nM insulin.*** Chronic exposure to nutrient stress results in a reduction of insulin-stimulated tyrosine phosphorylation at the level of IR-β and IRS-1, without affecting insulin-stimulated Ser^{473} Akt phosphorylation or adipogenesis. IRS-1 is more sensitive to this nutrient stress than IR-β, and possible mechanisms behind the attenuation of IR-β/IRS-1 may involve the induction of serine kinases and/or protein tyrosine phosphatases (see text for details). Changes in colour from green to red, and decreases in the phosphotyrosine symbol size, indicate inhibition.

CONCLUSION

This thesis focuses on the effect of chronic insulin and high glucose-based nutrient stress on human primary preadipocytes and their insulin-stimulated responses. Chronic exposure of preadipocytes to 25 mM glucose and 0.6 nM insulin for 48 hours inhibits insulin-stimulated IR-β and IRS-1 Tyr phosphorylation. IRS-1 Tyr phosphorylation was more sensitive to this stress compared that of IR-β, since either 25 mM glucose or 0.6 nM insulin alone attenuated insulin-stimulated Tyr phosphorylation. Furthermore, 25 mM glucose or 0.6 nM individually, generated a similar inhibitory effect on IRS-1 Tyr phosphorylation as the combination of the two. In contrast, insulin-stimulated Ser^{473} phosphorylation of Akt was not inhibited by chronic exposure to 25 mM glucose and/or 0.6 nM insulin. Similarly, the expression of pro-inflammatory adipokines was unchanged by these conditions. Finally, despite the inhibition of acute insulin signaling at the level of IR-β and IRS-1, nutrient stress prior to and/or during differentiation did not alter TG accumulation or adipogenic protein expression.

The adipogenic potential and size of the preadipocyte pool *in vivo* determines whether hypertrophic versus hyperplastic expansion occurs. Extrapolated to an *in vivo* setting, my findings suggest that chronic 0.6 nM insulin and high glucose-based stress may not impair the role of the preadipocyte in AT remodeling. My studies add further information about the preadipocyte and its role in AT remodeling and dysfunction under conditions of nutrient stress.

REFERENCES

Ahima, R.S., and Lazar, M.A. (2013). Physiology. The health risk of obesity--better metrics imperative. Science *341,* 856-858.

Alhusaini, S., McGee, K., Schisano, B., Harte, A., McTernan, P., Kumar, S., and Tripathi, G. (2010). Lipopolysaccharide, high glucose and saturated fatty acids induce endoplasmic reticulum stress in cultured primary human adipocytes: Salicylate alleviates this stress. Biochem. Biophys. Res. Commun. *397,* 472-478.

Aratani, Y., and Kitagawa, Y. (1988). Enhanced synthesis and secretion of type IV collagen and entactin during adipose conversion of 3T3-L1 cells and production of unorthodox laminin complex. J. Biol. Chem. *263,* 16163-16169.

Armoni, M., Harel, C., Karni, S., Chen, H., Bar-Yoseph, F., Ver, M.R., Quon, M.J., and Karnieli, E. (2006). FOXO1 represses peroxisome proliferator-activated receptor-gamma1 and -gamma2 gene promoters in primary adipocytes. A novel paradigm to increase insulin sensitivity. J. Biol. Chem. *281,* 19881-19891.

Arner, E., Westermark, P.O., Spalding, K.L., Britton, T., Ryden, M., Frisen, J., Bernard, S., and Arner, P. (2010). Adipocyte turnover: relevance to human adipose tissue morphology. Diabetes *59,* 105-109.

Back, K., and Arnqvist, H.J. (2009). Changes in insulin and IGF-I receptor expression during differentiation of human preadipocytes. Growth Horm. IGF Res. *19,* 101-111.

Bae, K.H., Kim, W.K., and Lee, S.C. (2012). Involvement of protein tyrosine phosphatases in adipogenesis: new anti-obesity targets? BMB Rep. *45,* 700-706.

Belfiore, A., Frasca, F., Pandini, G., Sciacca, L., and Vigneri, R. (2009). Insulin receptor isoforms and insulin receptor/insulin-like growth factor receptor hybrids in physiology and disease. Endocr. Rev. *30,* 586-623.

Berry, R., and Rodeheffer, M.S. (2013). Characterization of the adipocyte cellular lineage in vivo. Nat. Cell Biol. *15,* 302-308.

Berti, L., Mosthaf, L., Kroder, G., Kellerer, M., Tippmer, S., Mushack, J., Seffer, E., Seedorf, K., and Haring, H. (1994). Glucose-induced translocation of protein kinase C isoforms in rat-1 fibroblasts is paralleled by inhibition of the insulin receptor tyrosine kinase. J. Biol. Chem. *269,* 3381-3386.

Blakesley, V.A., Scrimgeour, A., Esposito, D., and Le Roith, D. (1996). Signaling via the insulin-like growth factor-I receptor: does it differ from insulin receptor signaling? Cytokine Growth Factor Rev. *7,* 153-159.

Bluher, M. (2010). The distinction of metabolically 'healthy' from 'unhealthy' obese individuals. Curr. Opin. Lipidol. *21,* 38-43.

Bollag, G.E., Roth, R.A., Beaudoin, J., Mochly-Rosen, D., and Koshland, D.E.,Jr. (1986). Protein kinase C directly phosphorylates the insulin receptor in vitro and reduces its protein-tyrosine kinase activity. Proc. Natl. Acad. Sci. U. S. A. *83,* 5822-5824.

Boucher, J., Kleinridders, A., and Kahn, C.R. (2014). Insulin receptor signaling in normal and insulin-resistant states. Cold Spring Harb Perspect. Biol. *6,* 10.1101/cshperspect.a009191.

Boura-Halfon, S., and Zick, Y. (2009). Phosphorylation of IRS proteins, insulin action, and insulin resistance. Am. J. Physiol. Endocrinol. Metab. *296,* E581-91.

Bourin, P., Bunnell, B.A., Casteilla, L., Dominici, M., Katz, A.J., March, K.L., Redl, H., Rubin, J.P., Yoshimura, K., and Gimble, J.M. (2013). Stromal cells from the adipose tissue-derived stromal vascular fraction and culture expanded adipose tissue-derived stromal/stem cells: a joint statement of the International Federation for Adipose Therapeutics and Science (IFATS) and the International Society for Cellular Therapy (ISCT). Cytotherapy *15,* 641-648.

Bowers, R.R., and Lane, M.D. (2008). Wnt signaling and adipocyte lineage commitment. Cell. Cycle *7,* 1191-1196.

Buren, J., Liu, H.X., Lauritz, J., and Eriksson, J.W. (2003). High glucose and insulin in combination cause insulin receptor substrate-1 and -2 depletion and protein kinase B desensitisation in primary cultured rat adipocytes: possible implications for insulin resistance in type 2 diabetes. Eur. J. Endocrinol. *148,* 157-167.

Cassese, A., Esposito, I., Fiory, F., Barbagallo, A.P., Paturzo, F., Mirra, P., Ulianich, L., Giacco, F., Iadicicco, C., Lombardi, A.*, et al.* (2008). In skeletal muscle advanced glycation end products (AGEs) inhibit insulin action and induce the formation of multimolecular complexes including the receptor for AGEs. J. Biol. Chem. *283,* 36088-36099.

Catalano, K.J., Maddux, B.A., Szary, J., Youngren, J.F., Goldfine, I.D., and Schaufele, F. (2014). Insulin resistance induced by hyperinsulinemia coincides with a persistent alteration at the insulin receptor tyrosine kinase domain. PLoS One *9,* e108693.

Cawthorn, W.P., Bree, A.J., Yao, Y., Du, B., Hemati, N., Martinez-Santibanez, G., and MacDougald, O.A. (2012). Wnt6, Wnt10a and Wnt10b inhibit adipogenesis and stimulate osteoblastogenesis through a beta-catenin-dependent mechanism. Bone *50,* 477-489.

Choi, S.M., Tucker, D.F., Gross, D.N., Easton, R.M., DiPilato, L.M., Dean, A.S., Monks, B.R., and Birnbaum, M.J. (2010). Insulin regulates adipocyte lipolysis via an Akt-independent signaling pathway. Mol. Cell. Biol. *30,* 5009-5020.

Collins, J.M., Neville, M.J., Pinnick, K.E., Hodson, L., Ruyter, B., van Dijk, T.H., Reijngoud, D.J., Fielding, M.D., and Frayn, K.N. (2011). De novo lipogenesis in the differentiating human adipocyte can provide all fatty acids necessary for maturation. J. Lipid Res. *52,* 1683-1692.

Constant, V.A., Gagnon, A., Landry, A., and Sorisky, A. (2006). Macrophage-conditioned medium inhibits the differentiation of 3T3-L1 and human abdominal preadipocytes. Diabetologia *49,* 1402-1411.

Copps, K.D., and White, M.F. (2012). Regulation of insulin sensitivity by serine/threonine phosphorylation of insulin receptor substrate proteins IRS1 and IRS2. Diabetologia *55,* 2565-2582.

Cristancho, A.G., and Lazar, M.A. (2011). Forming functional fat: a growing understanding of adipocyte differentiation. Nat. Rev. Mol. Cell Biol. *12,* 722-734.

Crossno, J.T.,Jr, Majka, S.M., Grazia, T., Gill, R.G., and Klemm, D.J. (2006). Rosiglitazone promotes development of a novel adipocyte population from bone marrow-derived circulating progenitor cells. J. Clin. Invest. *116,* 3220-3228.

Danielsson, A., Nystrom, F.H., and Stralfors, P. (2006). Phosphorylation of IRS1 at serine 307 and serine 312 in response to insulin in human adipocytes. Biochem. Biophys. Res. Commun. *342,* 1183-1187.

De Meyts, P., Sajid, W., Palsgaard, J., Theede, A., Gauguin, L., Aladdin, H., and Whittaker, J. (2000). Insulin and IGF-I Receptor Structure and Binding Mechanism.

Draznin, B. (2006). Molecular mechanisms of insulin resistance: serine phosphorylation of insulin receptor substrate-1 and increased expression of p85alpha: the two sides of a coin. Diabetes *55,* 2392-2397.

Du, Y., and Wei, T. (2014). Inputs and outputs of insulin receptor. Protein Cell. *5,* 203-213.

Entenmann, G., and Hauner, H. (1996). Relationship between replication and differentiation in cultured human adipocyte precursor cells. Am. J. Physiol. *270,* C1011-6.

Esser, N., Legrand-Poels, S., Piette, J., Scheen, A.J., and Paquot, N. (2014). Inflammation as a link between obesity, metabolic syndrome and type 2 diabetes. Diabetes Res. Clin. Pract. *105,* 141-150.

Fajas, L., Schoonjans, K., Gelman, L., Kim, J.B., Najib, J., Martin, G., Fruchart, J.C., Briggs, M., Spiegelman, B.M., and Auwerx, J. (1999). Regulation of peroxisome proliferator-activated receptor gamma expression by adipocyte differentiation and determination factor 1/sterol regulatory element binding protein 1: implications for adipocyte differentiation and metabolism. Mol. Cell. Biol. *19,* 5495-5503.

Fan, W., Imamura, T., Sonoda, N., Sears, D.D., Patsouris, D., Kim, J.J., and Olefsky, J.M. (2009). FOXO1 transrepresses peroxisome proliferator-activated receptor gamma transactivation, coordinating an insulin-induced feed-forward response in adipocytes. J. Biol. Chem. *284,* 12188-12197.

Farmer, S.R. (2006). Transcriptional control of adipocyte formation. Cell. Metab. *4,* 263-273.

Filippis, A., Clark, S., and Proietto, J. (1997). Increased flux through the hexosamine biosynthesis pathway inhibits glucose transport acutely by activation of protein kinase C. Biochem. J. *324 (Pt 3),* 981-985.

Frayn, K.N. (2002). Adipose tissue as a buffer for daily lipid flux. Diabetologia *45,* 1201-1210.

Freidenberg, G.R., Henry, R.R., Klein, H.H., Reichart, D.R., and Olefsky, J.M. (1987). Decreased kinase activity of insulin receptors from adipocytes of non-insulin-dependent diabetic subjects. J. Clin. Invest. *79,* 240-250.

Fruhbeck, G., Mendez-Gimenez, L., Fernandez-Formoso, J.A., Fernandez, S., and Rodriguez, A. (2014). Regulation of adipocyte lipolysis. Nutr. Res. Rev. *27,* 63-93.

Gagnon, A., and Sorisky, A. (1998). The effect of glucose concentration on insulin-induced 3T3-L1 adipose cell differentiation. Obes. Res. *6,* 157-163.

Gao, C.L., Zhu, C., Zhao, Y.P., Chen, X.H., Ji, C.B., Zhang, C.M., Zhu, J.G., Xia, Z.K., Tong, M.L., and Guo, X.R. (2010). Mitochondrial dysfunction is induced by high levels of glucose and free fatty acids in 3T3-L1 adipocytes. Mol. Cell. Endocrinol. *320,* 25-33.

Gathercole, L.L., Morgan, S.A., Bujalska, I.J., Hauton, D., Stewart, P.M., and Tomlinson, J.W. (2011). Regulation of lipogenesis by glucocorticoids and insulin in human adipose tissue. PLoS One *6,* e26223.

Gathercole, L.L., Morgan, S.A., and Tomlinson, J.W. (2013). Hormonal regulation of lipogenesis. Vitam. Horm. *91,* 1-27.

Gavin, J.R.,3rd, Roth, J., Neville, D.M.,Jr, de Meyts, P., and Buell, D.N. (1974). Insulin-dependent regulation of insulin receptor concentrations: a direct demonstration in cell culture. Proc. Natl. Acad. Sci. U. S. A. *71,* 84-88.

Gesta, S., Bluher, M., Yamamoto, Y., Norris, A.W., Berndt, J., Kralisch, S., Boucher, J., Lewis, C., and Kahn, C.R. (2006). Evidence for a role of developmental genes in the origin of obesity and body fat distribution. Proc. Natl. Acad. Sci. U. S. A. *103,* 6676-6681.

Golan, D., and Tashjian, A. (2012). Principles of pharmacology : the pathophysiologic basis of drug therapy. (Philadelphia: Wolters Kluwer Health/Lippincott Williams & Wilkins) pp. 529.

Green, H., and Kehinde, O. (1975). An established preadipose cell line and its differentiation in culture. II. Factors affecting the adipose conversion. Cell *5,* 19-27.

Greene, E.L., Nelson, B.A., Robinson, K.A., and Buse, M.G. (2001). alpha-Lipoic acid prevents the development of glucose-induced insulin resistance in 3T3-L1 adipocytes and accelerates the decline in immunoreactive insulin during cell incubation. Metabolism *50,* 1063-1069.

Grygiel-Gorniak, B. (2014). Peroxisome proliferator-activated receptors and their ligands: nutritional and clinical implications--a review. Nutr. J. *13,* 17-2891-13-17.

Gurzov, E.N., Stanley, W.J., Brodnicki, T.C., and Thomas, H.E. (2015). Protein tyrosine phosphatases: molecular switches in metabolism and diabetes. Trends Endocrinol. Metab. *26,* 30-39.

Haber, C.A., Lam, T.K., Yu, Z., Gupta, N., Goh, T., Bogdanovic, E., Giacca, A., and Fantus, I.G. (2003). N-acetylcysteine and taurine prevent hyperglycemia-induced insulin resistance in vivo: possible role of oxidative stress. Am. J. Physiol. Endocrinol. Metab. *285,* E744-53.

Han, C.Y., Subramanian, S., Chan, C.K., Omer, M., Chiba, T., Wight, T.N., and Chait, A. (2007). Adipocyte-derived serum amyloid A3 and hyaluronan play a role in monocyte recruitment and adhesion. Diabetes *56,* 2260-2273.

Hancer, N.J., Qiu, W., Cherella, C., Li, Y., Copps, K.D., and White, M.F. (2014). Insulin and metabolic stress stimulate multisite serine/threonine phosphorylation of insulin receptor substrate 1 and inhibit tyrosine phosphorylation. J. Biol. Chem. *289,* 12467-12484.

Hassan, M., Latif, N., and Yacoub, M. (2012). Adipose tissue: friend or foe? Nat. Rev. Cardiol. *9,* 689-702.

Hauner, H. (2005). Secretory factors from human adipose tissue and their functional role. Proc. Nutr. Soc. *64,* 163-169.

Hauner, H., Rohrig, K., Spelleken, M., Liu, L.S., and Eckel, J. (1998). Development of insulin-responsive glucose uptake and GLUT4 expression in differentiating human adipocyte precursor cells. Int. J. Obes. Relat. Metab. Disord. *22,* 448-453.

Hauner, H., Wabitsch, M., and Pfeiffer, E.F. (1988). Differentiation of adipocyte precursor cells from obese and nonobese adult women and from different adipose tissue sites. Horm. Metab. Res. Suppl. *19,* 35-39.

Hoffman, J.M., Ishizuka, T., and Farese, R.V. (1991). Interrelated effects of insulin and glucose on diacylglycerol-protein kinase-C signalling in rat adipocytes and solei muscle in vitro and in vivo in diabetic rats. Endocrinology *128,* 2937-2948.

Hua, Q. (2010). Insulin: a small protein with a long journey. Protein Cell. *1,* 537-551.

Huang, H.Y., Hu, L.L., Song, T.J., Li, X., He, Q., Sun, X., Li, Y.M., Lu, H.J., Yang, P.Y., and Tang, Q.Q. (2011). Involvement of cytoskeleton-associated proteins in the commitment of C3H10T1/2 pluripotent stem cells to adipocyte lineage induced by BMP2/4. Mol. Cell. Proteomics *10,* M110.002691.

Ibrahim, M.M. (2010). Subcutaneous and visceral adipose tissue: structural and functional differences. Obes. Rev. *11,* 11-18.

Idris, I., Gray, S., and Donnelly, R. (2001). Protein kinase C activation: isozyme-specific effects on metabolism and cardiovascular complications in diabetes. Diabetologia *44,* 659-673.

Jeffery, E., Church, C.D., Holtrup, B., Colman, L., and Rodeheffer, M.S. (2015). Rapid depot-specific activation of adipocyte precursor cells at the onset of obesity. Nat. Cell Biol. *17,* 376-385.

Ji, E., Jung, M.Y., Park, J.H., Kim, S., Seo, C.R., Park, K.W., Lee, E.K., Yeom, C.H., and Lee, S. (2014). Inhibition of adipogenesis in 3T3-L1 cells and suppression of abdominal fat accumulation in high-fat diet-feeding C57BL/6J mice after downregulation of hyaluronic acid. Int. J. Obes. (Lond) *38,* 1035-1043.

Jung, U.J., and Choi, M.S. (2014). Obesity and its metabolic complications: the role of adipokines and the relationship between obesity, inflammation, insulin resistance, dyslipidemia and nonalcoholic fatty liver disease. Int. J. Mol. Sci. *15,* 6184-6223.

Kajimura, S., and Saito, M. (2014). A new era in brown adipose tissue biology: molecular control of brown fat development and energy homeostasis. Annu. Rev. Physiol. *76,* 225-249.

Karbowska, J., and Kochan, Z. (2006). Role of adiponectin in the regulation of carbohydrate and lipid metabolism. J. Physiol. Pharmacol. *57 Suppl 6,* 103-113.

Khan, M., and Joseph, F. (2014). Adipose tissue and adipokines: the association with and application of adipokines in obesity. Scientifica (Cairo) *2014,* 328592.

Kim, J.B., Wright, H.M., Wright, M., and Spiegelman, B.M. (1998). ADD1/SREBP1 activates PPARgamma through the production of endogenous ligand. Proc. Natl. Acad. Sci. U. S. A. *95,* 4333-4337.

Kim, S.M., Lun, M., Wang, M., Senyo, S.E., Guillermier, C., Patwari, P., and Steinhauser, M.L. (2014). Loss of white adipose hyperplastic potential is associated with enhanced susceptibility to insulin resistance. Cell. Metab. *20,* 1049-1058.

Koenen, T.B., Stienstra, R., van Tits, L.J., de Graaf, J., Stalenhoef, A.F., Joosten, L.A., Tack, C.J., and Netea, M.G. (2011). Hyperglycemia activates caspase-1 and TXNIP-mediated IL-1beta transcription in human adipose tissue. Diabetes *60,* 517-524.

Kraakman, M.J., Murphy, A.J., Jandeleit-Dahm, K., and Kammoun, H.L. (2014). Macrophage polarization in obesity and type 2 diabetes: weighing down our understanding of macrophage function? Front. Immunol. *5,* 470.

Lacasa, D., Taleb, S., Keophiphath, M., Miranville, A., and Clement, K. (2007). Macrophage-secreted factors impair human adipogenesis: involvement of proinflammatory state in preadipocytes. Endocrinology *148,* 868-877.

Laemmli, U.K. (1970). Cleavage of structural proteins during the assembly of the head of bacteriophage T4. Nature *227,* 680-685.

Lee, M.J., Wu, Y., and Fried, S.K. (2013). Adipose tissue heterogeneity: implication of depot differences in adipose tissue for obesity complications. Mol. Aspects Med. *34,* 1-11.

Lessard, J., Laforest, S., Pelletier, M., Leboeuf, M., Blackburn, L., and Tchernof, A. (2014). Low abdominal subcutaneous preadipocyte adipogenesis is associated with visceral obesity, visceral adipocyte hypertrophy, and a dysmetabolic state. Adipocyte *3,* 197-205.

Lima, F.B., Thies, R.S., and Garvey, W.T. (1991). Glucose and insulin regulate insulin sensitivity in primary cultured adipocytes without affecting insulin receptor kinase activity. Endocrinology *128,* 2415-2426.

Lin, Y., Berg, A.H., Iyengar, P., Lam, T.K., Giacca, A., Combs, T.P., Rajala, M.W., Du, X., Rollman, B., Li, W.*, et al.* (2005). The hyperglycemia-induced inflammatory response in adipocytes: the role of reactive oxygen species. J. Biol. Chem. *280,* 4617-4626.

Ling, H.Y., Hu, B., Hu, X.B., Zhong, J., Feng, S.D., Qin, L., Liu, G., Wen, G.B., and Liao, D.F. (2012). MiRNA-21 reverses high glucose and high insulin induced insulin resistance in 3T3-L1 adipocytes through targeting phosphatase and tensin homologue. Exp. Clin. Endocrinol. Diabetes *120,* 553-559.

Liu, J., Desai, K., Wang, R., and Wu, L. (2013). Up-regulation of aldolase A and methylglyoxal production in adipocytes. Br. J. Pharmacol. *168,* 1639-1646.

Liu, X., Wang, S., You, Y., Meng, M., Zheng, Z., Dong, M., Lin, J., Zhao, Q., Zhang, C., Yuan, X.*, et al.* (2015). Brown Adipose Tissue Transplantation Reverses Obesity in Ob/Ob Mice. Endocrinology *156,* 2461-2469.

Lu, Q., Li, M., Zou, Y., and Cao, T. (2014). Induction of adipocyte hyperplasia in subcutaneous fat depot alleviated type 2 diabetes symptoms in obese mice. Obesity (Silver Spring) *22,* 1623-1631.

Maegawa, H., Ide, R., Hasegawa, M., Ugi, S., Egawa, K., Iwanishi, M., Kikkawa, R., Shigeta, Y., and Kashiwagi, A. (1995). Thiazolidine derivatives ameliorate high glucose-induced insulin resistance via the normalization of protein-tyrosine phosphatase activities. J. Biol. Chem. *270,* 7724-7730.

Marshall, S., and Olefsky, J.M. (1980). Effects of insulin incubation on insulin binding, glucose transport, and insulin degradation by isolated rat adipocytes. Evidence for hormone-induced desensitization at the receptor and postreceptor level. J. Clin. Invest. *66,* 763-772.

Martyn, J.A., Kaneki, M., and Yasuhara, S. (2008). Obesity-induced insulin resistance and hyperglycemia: etiologic factors and molecular mechanisms. Anesthesiology *109,* 137-148.

Mehran, A.E., Templeman, N.M., Brigidi, G.S., Lim, G.E., Chu, K.Y., Hu, X., Botezelli, J.D., Asadi, A., Hoffman, B.G., Kieffer, T.J.*, et al.* (2012). Hyperinsulinemia drives diet-induced obesity independently of brain insulin production. Cell. Metab. *16,* 723-737.

Miki, H., Yamauchi, T., Suzuki, R., Komeda, K., Tsuchida, A., Kubota, N., Terauchi, Y., Kamon, J., Kaburagi, Y., Matsui, J.*, et al.* (2001). Essential role of insulin receptor substrate 1 (IRS-1) and IRS-2 in adipocyte differentiation. Mol. Cell. Biol. *21,* 2521-2532.

Mills, C.D. (2012). M1 and M2 Macrophages: Oracles of Health and Disease. Crit. Rev. Immunol. *32,* 463-488.

Moreno-Navarrete, J.M., Ortega, F., Sanchez-Garrido, M.A., Sabater, M., Ricart, W., Zorzano, A., Tena-Sempere, M., and Fernandez-Real, J.M. (2013). Phosphorylated S6K1 (Thr389) is a molecular adipose tissue marker of altered glucose tolerance. J. Nutr. Biochem. *24,* 32-38.

Mussig, K., Staiger, H., Fiedler, H., Moeschel, K., Beck, A., Kellerer, M., and Haring, H.U. (2005). Shp2 is required for protein kinase C-dependent phosphorylation of serine 307 in insulin receptor substrate-1. J. Biol. Chem. *280,* 32693-32699.

Nelson, B.A., Robinson, K.A., and Buse, M.G. (2002). Defective Akt activation is associated with glucose- but not glucosamine-induced insulin resistance. Am. J. Physiol. Endocrinol. Metab. *282,* E497-506.

Nelson, B.A., Robinson, K.A., and Buse, M.G. (2000). High glucose and glucosamine induce insulin resistance via different mechanisms in 3T3-L1 adipocytes. Diabetes *49,* 981-991.

Nye, C.K., Hanson, R.W., and Kalhan, S.C. (2008). Glyceroneogenesis is the dominant pathway for triglyceride glycerol synthesis in vivo in the rat. J. Biol. Chem. *283,* 27565-27574.

O'Connell, J., Lynch, L., Cawood, T.J., Kwasnik, A., Nolan, N., Geoghegan, J., McCormick, A., O'Farrelly, C., and O'Shea, D. (2010). The relationship of omental and subcutaneous adipocyte size to metabolic disease in severe obesity. PLoS One *5,* e9997.

Odegaard, J.I., and Chawla, A. (2013). Pleiotropic actions of insulin resistance and inflammation in metabolic homeostasis. Science *339,* 172-177.

Onate, B., Vilahur, G., Ferrer-Lorente, R., Ybarra, J., Diez-Caballero, A., Ballesta-Lopez, C., Moscatiello, F., Herrero, J., and Badimon, L. (2012). The subcutaneous adipose tissue reservoir of functionally active stem cells is reduced in obese patients. FASEB J. *26,* 4327-4336.

Ong, W.K., Tan, C.S., Chan, K.L., Goesantoso, G.G., Chan, X.H., Chan, E., Yin, J., Yeo, C.R., Khoo, C.M., So, J.B.*, et al.* (2014). Identification of specific cell-surface markers of adipose-derived stem cells from subcutaneous and visceral fat depots. Stem Cell. Reports *2,* 171-179.

Otto, T.C., and Lane, M.D. (2005). Adipose development: from stem cell to adipocyte. Crit. Rev. Biochem. Mol. Biol. *40,* 229-242.

Pan, Z., Wang, H., Liu, Y., Yu, C., Zhang, Y., Chen, J., Wang, X., and Guan, Q. (2014). Involvement of CSE/ H2S in high glucose induced aberrant secretion of adipokines in 3T3-L1 adipocytes. Lipids Health. Dis. *13,* 155-511X-13-155.

Parlee, S.D., Lentz, S.I., Mori, H., and MacDougald, O.A. (2014). Quantifying size and number of adipocytes in adipose tissue. Methods Enzymol. *537,* 93-122.

Paz, K., Hemi, R., LeRoith, D., Karasik, A., Elhanany, E., Kanety, H., and Zick, Y. (1997). A molecular basis for insulin resistance. Elevated serine/threonine phosphorylation of IRS-1 and IRS-2 inhibits their binding to the juxtamembrane region of the insulin receptor and impairs their ability to undergo insulin-induced tyrosine phosphorylation. J. Biol. Chem. *272,* 29911-29918.

Paz, K., Liu, Y.F., Shorer, H., Hemi, R., LeRoith, D., Quan, M., Kanety, H., Seger, R., and Zick, Y. (1999). Phosphorylation of insulin receptor substrate-1 (IRS-1) by protein kinase B positively regulates IRS-1 function. J. Biol. Chem. *274,* 28816-28822.

Pedersen, D.J., Guilherme, A., Danai, L.V., Heyda, L., Matevossian, A., Cohen, J., Nicoloro, S.M., Straubhaar, J., Noh, H.L., Jung, D., Kim, J.K., and Czech, M.P. (2015). A major role of insulin in promoting obesity-associated adipose tissue inflammation. Mol. Metab. *4,* 507-518.

Pillay, T.S., Xiao, S., and Olefsky, J.M. (1996). Glucose-induced phosphorylation of the insulin receptor. Functional effects and characterization of phosphorylation sites. J. Clin. Invest. *97,* 613-620.

Prasad, I., Zouzias, D., and Basilico, C. (1976). State of the viral DNA in rat cells transformed by polyoma virus. I. Virus rescue and the presence of nonintergrated viral DNA molecules. J. Virol. *18,* 436-444.

Proenca, A.R., Sertie, R.A., Oliveira, A.C., Campaaa, A.B., Caminhotto, R.O., Chimin, P., and Lima, F.B. (2014). New concepts in white adipose tissue physiology. Braz. J. Med. Biol. Res. *0,* 0.

Ramalingam, L., Oh, E., and Thurmond, D.C. (2013). Novel roles for insulin receptor (IR) in adipocytes and skeletal muscle cells via new and unexpected substrates. Cell Mol. Life Sci. *70,* 2815-2834.

Renstrom, F., Buren, J., Svensson, M., and Eriksson, J.W. (2007). Insulin resistance induced by high glucose and high insulin precedes insulin receptor substrate 1 protein depletion in human adipocytes. Metabolism *56,* 190-198.

Reznikoff, C.A., Brankow, D.W., and Heidelberger, C. (1973). Establishment and characterization of a cloned line of C3H mouse embryo cells sensitive to postconfluence inhibition of division. Cancer Res. *33,* 3231-3238.

Riboulet-Chavey, A., Pierron, A., Durand, I., Murdaca, J., Giudicelli, J., and Van Obberghen, E. (2006). Methylglyoxal impairs the insulin signaling pathways independently of the formation of intracellular reactive oxygen species. Diabetes *55,* 1289-1299.

Roberts, R., Hodson, L., Dennis, A.L., Neville, M.J., Humphreys, S.M., Harnden, K.E., Micklem, K.J., and Frayn, K.N. (2009). Markers of de novo lipogenesis in adipose tissue: associations with small adipocytes and insulin sensitivity in humans. Diabetologia *52,* 882-890.

Robinson, K.A., and Buse, M.G. (2008). Mechanisms of high-glucose/insulin-mediated desensitization of acute insulin-stimulated glucose transport and Akt activation. Am. J. Physiol. Endocrinol. Metab. *294,* E870-81.

Robinson, K.A., Hegyi, K., Hannun, Y.A., Buse, M.G., and Sethi, J.K. (2014). Go-6976 reverses hyperglycemia-induced insulin resistance independently of cPKC inhibition in adipocytes. PLoS One *9,* e108963.

Rogers, N.H. (2015). Brown adipose tissue during puberty and with aging. Ann. Med. *47,* 142-149.

Rosen, E.D., Sarraf, P., Troy, A.E., Bradwin, G., Moore, K., Milstone, D.S., Spiegelman, B.M., and Mortensen, R.M. (1999). PPAR gamma is required for the differentiation of adipose tissue in vivo and in vitro. Mol. Cell *4,* 611-617.

Rosen, E.D., and Spiegelman, B.M. (2014). What we talk about when we talk about fat. Cell *156,* 20-44.

Ross, S.A., Chen, X., Hope, H.R., Sun, S., McMahon, E.G., Broschat, K., and Gulve, E.A. (2000). Development and comparison of two 3T3-L1 adipocyte models of insulin resistance: increased glucose flux vs glucosamine treatment. Biochem. Biophys. Res. Commun. *273,* 1033-1041.

Samuel, V.T., and Shulman, G.I. (2012). Mechanisms for insulin resistance: common threads and missing links. Cell *148,* 852-871.

Sengenes, C., Lolmede, K., Zakaroff-Girard, A., Busse, R., and Bouloumie, A. (2005). Preadipocytes in the human subcutaneous adipose tissue display distinct features from the adult mesenchymal and hematopoietic stem cells. J. Cell. Physiol. *205,* 114-122.

Sera, Y., LaRue, A.C., Moussa, O., Mehrotra, M., Duncan, J.D., Williams, C.R., Nishimoto, E., Schulte, B.A., Watson, P.M., Watson, D.K., and Ogawa, M. (2009). Hematopoietic stem cell origin of adipocytes. Exp. Hematol. *37,* 1108-20, 1120.e1-4.

Shah, A., Mehta, N., and Reilly, M.P. (2008). Adipose inflammation, insulin resistance, and cardiovascular disease. JPEN J. Parenter. Enteral Nutr. *32,* 638-644.

Shimano, H. (2001). Sterol regulatory element-binding proteins (SREBPs): transcriptional regulators of lipid synthetic genes. Prog. Lipid Res. *40,* 439-452.

Shimizu, S., Maegawa, H., Egawa, K., Shi, K., Bryer-Ash, M., and Kashiwagi, A. (2002). Mechanism for differential effect of protein-tyrosine phosphatase 1B on Akt versus mitogen-activated protein kinase in 3T3-L1 adipocytes. Endocrinology *143,* 4563-4569.

Silva, K.R., Liechocki, S., Carneiro, J.R., Claudio-da-Silva, C., Maya-Monteiro, C.M., Borojevic, R., and Baptista, L.S. (2015). Stromal-vascular fraction content and adipose stem cell behavior are altered in morbid obese and post bariatric surgery ex-obese women. Stem Cell. Res. Ther. *6,* 72-015-0029-x.

Skurk, T., and Hauner, H. (2012). Primary culture of human adipocyte precursor cells: expansion and differentiation. Methods Mol. Biol. *806,* 215-226.

Slaaby, R. (2015). Specific insulin/IGF1 hybrid receptor activation assay reveals IGF1 as a more potent ligand than insulin. Sci. Rep. *5,* 7911.

Smith, N.C., Fairbridge, N.A., Pallegar, N.K., and Christian, S.L. (2015). Dynamic upregulation of CD24 in pre-adipocytes promotes adipogenesis. Adipocyte *4,* 89-100.

Snijder, M.B., Visser, M., Dekker, J.M., Goodpaster, B.H., Harris, T.B., Kritchevsky, S.B., De Rekeneire, N., Kanaya, A.M., Newman, A.B., Tylavsky, F.A., Seidell, J.C., and Health ABC Study. (2005). Low subcutaneous thigh fat is a risk factor for unfavourable glucose and lipid levels, independently of high abdominal fat. The Health ABC Study. Diabetologia *48,* 301-308.

Spalding, K.L., Arner, E., Westermark, P.O., Bernard, S., Buchholz, B.A., Bergmann, O., Blomqvist, L., Hoffstedt, J., Naslund, E., Britton, T.*, et al.* (2008). Dynamics of fat cell turnover in humans. Nature *453,* 783-787.

Spiegelman, B.M., Choy, L., Hotamisligil, G.S., Graves, R.A., and Tontonoz, P. (1993). Regulation of adipocyte gene expression in differentiation and syndromes of obesity/diabetes. J. Biol. Chem. *268,* 6823-6826.

Strissel, K.J., Stancheva, Z., Miyoshi, H., Perfield, J.W.,2nd, DeFuria, J., Jick, Z., Greenberg, A.S., and Obin, M.S. (2007). Adipocyte death, adipose tissue remodeling, and obesity complications. Diabetes *56,* 2910-2918.

Sun, K., Kusminski, C.M., and Scherer, P.E. (2011). Adipose tissue remodeling and obesity. J. Clin. Invest. *121,* 2094-2101.

Tang, Q.Q., and Lane, M.D. (2012). Adipogenesis: from stem cell to adipocyte. Annu. Rev. Biochem. *81,* 715-736.

Tang, Q.Q., Otto, T.C., and Lane, M.D. (2004). Commitment of C3H10T1/2 pluripotent stem cells to the adipocyte lineage. Proc. Natl. Acad. Sci. U. S. A. *101,* 9607-9611.

Tang, Q.Q., Otto, T.C., and Lane, M.D. (2003). Mitotic clonal expansion: a synchronous process required for adipogenesis. Proc. Natl. Acad. Sci. U. S. A. *100,* 44-49.

Tang, S., Le-Tien, H., Goldstein, B.J., Shin, P., Lai, R., and Fantus, I.G. (2001). Decreased in situ insulin receptor dephosphorylation in hyperglycemia-induced insulin resistance in rat adipocytes. Diabetes *50,* 83-90.

Tanis, R.M., Piroli, G.G., Day, S.D., and Frizzell, N. (2015). The effect of glucose concentration and sodium phenylbutyrate treatment on mitochondrial bioenergetics and ER stress in 3T3-L1 adipocytes. Biochim. Biophys. Acta *1853,* 213-221.

Tchkonia, T., Tchoukalova, Y.D., Giorgadze, N., Pirtskhalava, T., Karagiannides, I., Forse, R.A., Koo, A., Stevenson, M., Chinnappan, D., Cartwright, A., Jensen, M.D., and Kirkland, J.L. (2005). Abundance of two human preadipocyte subtypes with distinct capacities for replication, adipogenesis, and apoptosis varies among fat depots. Am. J. Physiol. Endocrinol. Metab. *288,* E267-77.

Tchkonia, T., Thomou, T., Zhu, Y., Karagiannides, I., Pothoulakis, C., Jensen, M.D., and Kirkland, J.L. (2013). Mechanisms and metabolic implications of regional differences among fat depots. Cell. Metab. *17,* 644-656.

Tchoukalova, Y., Koutsari, C., and Jensen, M. (2007). Committed subcutaneous preadipocytes are reduced in human obesity. Diabetologia *50,* 151-157.

Tchoukalova, Y.D., Votruba, S.B., Tchkonia, T., Giorgadze, N., Kirkland, J.L., and Jensen, M.D. (2010). Regional differences in cellular mechanisms of adipose tissue gain with overfeeding. Proc. Natl. Acad. Sci. U. S. A. *107,* 18226-18231.

Teo, C.F., Wollaston-Hayden, E.E., and Wells, L. (2010). Hexosamine flux, the O-GlcNAc modification, and the development of insulin resistance in adipocytes. Mol. Cell. Endocrinol. *318,* 44-53.

Tomiyama, K., Murase, N., Stolz, D.B., Toyokawa, H., O'Donnell, D.R., Smith, D.M., Dudas, J.R., Rubin, J.P., and Marra, K.G. (2008). Characterization of transplanted green fluorescent protein+ bone marrow cells into adipose tissue. Stem Cells *26,* 330-338.

Topp, W.C. (1981). Normal rat cell lines deficient in nuclear thymidine kinase. Virology *113,* 408-411.

Tsou, R.C., and Bence, K.K. (2012). The Genetics of PTPN1 and Obesity: Insights from Mouse Models of Tissue-Specific PTP1B Deficiency. J. Obes. *2012,* 926857.

Tsuchiya, A., Kanno, T., and Nishizaki, T. (2013). PI3 kinase directly phosphorylates Akt1/2 at Ser473/474 in the insulin signal transduction pathway. J. Endocrinol. *220,* 49-59.

Vainshtein, I., Kovacina, K.S., and Roth, R.A. (2001). The insulin receptor substrate (IRS)-1 pleckstrin homology domain functions in downstream signaling. J. Biol. Chem. *276,* 8073-8078.

Venable, C.L., Frevert, E.U., Kim, Y.B., Fischer, B.M., Kamatkar, S., Neel, B.G., and Kahn, B.B. (2000). Overexpression of protein-tyrosine phosphatase-1B in adipocytes inhibits insulin-stimulated phosphoinositide 3-kinase activity without altering glucose transport or Akt/Protein kinase B activation. J. Biol. Chem. *275,* 18318-18326.

White, M.F., Livingston, J.N., Backer, J.M., Lauris, V., Dull, T.J., Ullrich, A., and Kahn, C.R. (1988). Mutation of the insulin receptor at tyrosine 960 inhibits signal transmission but does not affect its tyrosine kinase activity. Cell 54, 641-649.

WHO. (2015). Obesity and overweight : Fact Sheet N°311. World Health Organization

Wagner, M.J., Stacey, M.M., Liu, B.A., and Pawson, T. (2013). Molecular mechanisms of SH2- and PTB-domain-containing proteins in receptor tyrosine kinase signaling. Cold Spring Harb Perspect. Biol. *5,* a008987.

Xu, E., Schwab, M., and Marette, A. (2014). Role of protein tyrosine phosphatases in the modulation of insulin signaling and their implication in the pathogenesis of obesity-linked insulin resistance. Rev. Endocr Metab. Disord. *15,* 79-97.

Young, S.G., and Zechner, R. (2013). Biochemistry and pathophysiology of intravascular and intracellular lipolysis. Genes Dev. *27,* 459-484.

Zhande, R., Mitchell, J.J., Wu, J., and Sun, X.J. (2002). Molecular mechanism of insulin-induced degradation of insulin receptor substrate 1. Mol. Cell. Biol. *22,* 1016-1026.

Zhang, Y., Proenca, R., Maffei, M., Barone, M., Leopold, L., and Friedman, J.M. (1994). Positional cloning of the mouse obese gene and its human homologue. Nature *372,* 425-432.

CURRICULUM VITAE

EDUCATION

University of Ottawa, Ottawa ON 09/2013 – 09/2015
M.Sc. Biochemistry

University of Ottawa, Ottawa ON 09/2009 – 06/2013
Hon. B.Sc. Biochemistry, option in Microbiology and Immunology – Magna Cum Laude

RESEARCH EXPERIENCE

Faculty of Medicine – Department of Biochemistry, Microbiology and Immunology (BMI)
University of Ottawa, Ottawa ON

M.Sc. Student (In affiliation with the Ottawa Hospital Research Institute) 09/2013 – 09/2015
Supervisor: Dr. Alexander Sorisky
Detailing the effects of hyperglycemia on human adipose tissue development, dysfunction, and inflammation. I performed assays and tissue culture (human tissue from elective abdominal surgeries). Furthermore I assessed, improved, and executed a self-directed project. I presented my findings at lab meetings, departmental meetings, and to an international audience at the American Diabetes Association 75th Scientific Sessions conference.

Honors Project Student/Summer Research Technician 09/2012 – 08/2013
Supervisor: Prof. Illimar Altosaar
Fusarium graminearum susceptible and resistant maize proteome analysis. I conducted literature reviews, performed experiments, analyzed mass spectrometry data, applied bioinformatic/statistical tools (Perseus software), and wrote a manuscript.

Work Study Student 05/2012 – 08/2012
Supervisor: Prof. Illimar Altosaar
Starch-Granule associated protein (SGAP) sampling of Oriza sativa. I appraised literature, designed/performed experiments to optimize SGAP purification, and collaborated with lab-mates to troubleshoot experimental issues.

Undergraduate Research Opportunity Program (UROP) Scholar 01/2012 – 04/2012
Supervisor: Prof. Illimar Altosaar
Creating site-specific Bone Morphogenetic Protein 2 mutants. I performed plasmid mini-preps, DNA digests, and purified proteins. I explained and presented this project to an audience with varied scientific backgrounds (from layperson to expert).

WORK EXPERIENCE

Biochemistry Teaching Assistant 01/2015 – 04/2015
Biochemistry Help Desk (Francophone Section)
University of Ottawa, Ottawa ON
Explained and simplified scientific concepts to second year biochemistry students

IT Service Helpdesk 06/2011 – 07/2011
Algonquin College, Ottawa ON
Communicated with staff and students to diagnose, resolve issues pertaining to their electronic devices
Re-imaged computers, and ensured proper mobile and laptop set-up for clients.

AWARDS AND DISTINCTIONS

- Faculty of Graduate and Postgraduate Studies, BMI, and Graduate Student Association Travel Grants (2015)
- Queen Elizabeth II Graduate Scholarship in Science and Technology (2013-2015)
- University of Ottawa Excellence Scholarship (2013-2015)
- University of Ottawa Graduate Admission Scholarship (Declined- 2013-2015)
- University of Ottawa Renewable Scholarship (2012-2013)
- Deans Honor List (2012 and 2013)
- Undergraduate Research Opportunity Program (UROP) Award (2012)
- University of Ottawa Undergraduate Admission Scholarship (2009-2010)
- Registrar's Special Scholarship (2009-2010)
- Queen Elizabeth II Scholarships Aiming for the Top Bursary (2009-2010)

PUBLICATIONS

El Bilali J.,.Gagnon AM., Sorisky A. (2015). Exposure to Insulin and High Glucose Inhibits Insulin Signaling in Human Preadipocytes. Diabetes; *64 (S1)*: 210-211. (Abstract).

Zaidi M., El Bilali J., Koziol A., Ward T., Styles G., Greenham T., Faiella W., Son H., Wan S., Taga I., Altosaar I. (2012). Gene technology in agriculture, environment and biopharming: Beyond Bt-rice and building better breeding budgets for crops. Journal of Plant Biochemistry & Biotechnology, *21(S1)*:2-9.

PRESENTATIONS

Exposure to Insulin and High Glucose Inhibits Insulin Signaling in Human Preadipocytes.
Authors: El Bilali J., Gagnon AM., Sorisky A.

- Poster, *American Diabetes Association 75th Scientific Sessions*, Boston MA, June 8th 2015
- Oral, *BMI Seminar Day*, University of Ottawa, Ottawa ON, March 10th 2015
- Poster, *Ottawa Hospital Research Institute Research Day*, Ottawa ON, November 13th 2014
- Poster, *BMI Poster Day*, University of Ottawa, Ottawa ON, May 15th 2014

The expression of bone morphogenetic protein 2 (BMP2) mutant proteins in E. coli.
Authors: El Bilali J., Styles G. and Altosaar I.

- Poster, *UROP Symposium*, University of Ottawa, Ottawa ON, March 29th 2012

SOFTWARE SKILLS

- Microsoft Office Suite
- Minitab
- Perseus

CERTIFICATIONS

Emergency First Responder, CPR-C, First Aid, AED

LANGUAGES

English, French